國立臺灣大學醫學院分子醫學研究所

碩士論文

Institute of Molecular Medicine, National Taiwan University

Master Thesis

ADAR1於干擾素訊號路徑中角色的研究與探討

Roles of ADAR1 in IFN-signaling pathway

研究生：陳濬鬻

Graduate Student: Jung-Hung Chen

指導教授：呂勝春 教授

譚賢明 副教授

中華民國一零一年七月

July, 2012

國立臺灣大學碩士學位論文
口試委員會審定書

ADAR1 於干擾素訊號路徑中角色的研究與探討

Roles of ADAR1 in IFN-signaling pathway

本論文係 **陳濬贇** 君（學號 R99448016）在國立臺灣大學分子醫學研究所完成之碩士學位論文，於民國一〇一年七月十六日星期一承下列考試委員審查通過及口試及格，特此證明

口試委員：

譚定明 （簽名）

（指導教授）

譚定明　徐元中

包勝春

系主任、所長 （簽名）

致謝

首先由衷感謝我的指導教授呂勝春老師、譚賢明老師以及徐立中老師，三位老師不時地給予我研究上的指導和建議，並藉此訓練我的思維，讓我能思考的更為全面。此外也感謝老師對我的鼓勵，讓我對自己更有信心。也要感謝老師對我的包容，並一再的原諒我脫線的舉止。老師的身教和言教都會是我學習的楷模。

在分醫所的這段日子，雖然為了課業實驗必須要兩地奔波，但是現在回想起來到也是難忘的回憶，而且總認為這是值得的。感謝分醫所每一位老師對我的栽培，雖然自己還有很大的進步空間，但我自認這兩年來我成長、改變了許多。我對自己的期望不高，不會希冀分醫所以我為榮，只希望不要因為我而蒙羞就好。未來我也會鞭策自己，希望能成為更完整的人。

再次感謝譚老師以及劉軒學姊對我這個小學弟的照顧。感謝之立學長讓我成長的更為堅強，也感謝長青、昌政、俊勳學長與我討論實驗並跟我打哈哈。感謝佳玲和惠雯學姐在實驗上給予的教導，以及在我難過時的安慰與關心。感謝不時必須接收我嘲諷，但依然十分照顧我的鍾佩、孟樺、玟欣和釭屏。感謝羿君給予我的行政上的支持。感謝分醫所同學的幫忙，雖然我走得跌跌撞撞，還是要感謝你們的扶持，也恭喜我們終究是順利走過這兩年了。感謝睿源學長，你豐富了我的生活。感謝政諺、匡博、承桓給我的挖苦和鼓勵。謝謝你們大家。

最後，謹以此文獻給我摯愛的家人。謝謝老爸老媽老哥對我無條件的支持與包容，你們造就了我，也是我的依靠。

Contents

摘要

ADAR1 為一具有脫氨活性的酵素，能將雙股 RNA 上與胸苷酸配對的腺苷酸進行脫氨而形成肌苷酸。由於肌苷酸結構與鳥苷酸相似，這種核苷酸序列的改變可能影響到 RNA 的二級結構、RNA 的穩定性甚至是密碼子的組成，造成基因表現程度甚至是基因功能的改變。ADAR1 包含兩種蛋白異構體，分別為 ADAR1p150 和 ADAR1p110，其中 ADAR1p150 的表現會受到干擾素的訊號路徑刺激而增加，此外許多文獻指出病毒的 RNA 也會受到 ADAR1 的修飾。因此 ADAR1 被認為參與在干擾素的相關路徑當中，但是目前對於 ADAR1 在其中扮演的角色仍舊不是很清楚。在本篇研究中，我們利用 siRNA 抑制 ADAR1 的表現，證實 IFI27L1、IFNAR1、IFNAR2、 MAVS、 RIG-1 皆受到 ADAR1 的修飾，其中 IFI27L1 的 mRNA 有增加的趨勢。另一方面，PRKRA 的 mRNA 和蛋白質表現量有明顯的下降，而根據次世代定序資料庫的資訊，我們證實在 PRKRA 轉錄本的下游有一段與之重疊的反義轉錄本，同時此反義轉錄本也會受到 ADAR1 的修飾。我們發現當 ADAR1 的表現被抑制後，此反義轉錄本的表現量以及 RNA 半生期都有增加的趨勢。綜合上述結果，我們發現許多參與在 RLR 以及 JAK/STAT 訊號路徑的基因，都會受到 ADAR1 的修飾；此外我們推測 ADAR1 能藉由與反義轉錄本的相互作用，進而影響到相關基因的表現。

Abstract

ADAR1 enzyme catalyzes deamination of adenine(A) on double stranded RNA to yield inosine(I). Because inosine is recognized as guanine by cellular machineries, such ADAR1-meidated post-transcriptional nucleotide sequence modification can affect several gene expressions and biological processes. Several studies have demonstrated that, in addition to cellular targets, viral transcripts are substrates for ADAR1, and that ADAR1 exhibits both anti-viral and proviral activities. Interferon (IFN), acting as an antiviral agent, is known to induce the expression of ADAR1 p150 isoform, further suggesting that ADAR1 may be linked to the IFN signaling pathway; however, its roles in this regulation remains uncharacterized. Our recent deep sequencing approach of identifying gene targets of ADAR1 revealed several candidate genes with functions associated with RLR and JAK/STAT signaling. We tested and confirmed editing events and RNA expression level of IFI27L1, IFNAR1, IFNAR2, MAVS, RIG-1 and PRKRA. The A-to-I editing events are confirmed by Sanger sequencing, which further showed obvious ADAR1-dependent editing events in IFI27L1, IFNAR1, IFNAR2, MAVS and RIG-1. Furthermore, higher RNA expression level of IFI27L1 is detected in ADAR1 knockdown cells. With regard to the PRKRA transcript, our observation and sequencing data further imply that there is an anti-sense transcript overlapping with 3' end of the PRKRA gene locus and that RNA editing may be linked to its regulation. Intriguingly,

both mRNA as well as protein expression are decreased and half-life time of the antisense transcript is increased after ADAR1 knockdown. Based on these preliminary findings, we hypothesize that ADAR1 may affect these genes at post-transcriptional level, and in turn modulate the associated signaling pathway. Future work focused on dissecting the mechanism of ADAR1 function in RLR and JAK/STAT signaling as well as in the regulation of PRKRA expression is discussed.

1. Introduction

1.1 Adenosine deaminases acting on RNA (ADARs) family

ADARs are a kind of enzymes that behave RNA editing activity, which catalyze the deamination of adenine (A) to inosine (I) in a site specific or promiscuous way. Their catalytic activity is considered a way to promote complexity and diversity of RNA(Jantsch 2010; Wahlstedt and Ohman 2011; Orlandi, Barbon et al. 2012). Moreover, ADARs activities, including cellular localization, dimerization and interaction with other trans-components, are supposed to be regulated precisely by several mechanism(Orlandi, Barbon et al. 2012). There are three members belong to ADAR family, including ADAR1, ADAR2 and ADAR3. ADAR1 and ADAR2 are expressed in most tissues, especially in the brain; on the other hand, ADAR3 is expressed in central nervous system only. ADAR3 doesn't show deaminase activity although this protein contains a deaminase domain(Melcher, Maas et al. 1996; Melcher, Maas et al. 1996); for this reason, the biological function of ADAR3 is still not clear(Jin, Zhang et al. 2009; Zinshteyn and Nishikura 2009; Nishikura 2010). Based on the nucleotide and amino acid sequence, it seems that ADAR1 is involved in immune system(Garcia-Sastre 2011; Samuel 2011; Li, Okonski et al. 2012). ADAR1 has two subtypes, one is ADAR1p110 and the other one is ADAR1p150 actually(Patterson and Samuel 1995). The former is expressed constitutively; however the latter is driven

through an interferon-sensitive response elements (ISRE)(Ward, Markle et al. 2002; Garcia-Sastre 2011). Furthermore, according to the comparison information of the amino acid sequence of ADAR1 and ADAR2 demonstrate that both two proteins contain three structured regions, three middle RNA binding domains (RBDs), a nuclear localization sequence (NLS), and a RNA deaminase domain in C-terminal region(Samuel 2011). Interestingly, there is a nuclear export signal (NES) reside in N-terminal of ADAR1.

Because ADAR1p150 is turned on under IFN signaling pathway, and express their deaminase activity in cytoplasm, where viral replication occurs. In addition, it has been suggested that ADAR1p150 also participated in immune response. For these reasons, in this research we focus on the relationship between ADAR1p150 and target genes involved in immune-associated signaling pathways.

1.2 Retinoic acid-inducible gene I (RIG-I)-like receptor (RLR) signaling pathway

RIG-I protein is one of RLR family members, which recognizes cytosolic RNA and shows RNA helicase activity(Haller, Kochs et al. 2006; Wilkins and Gale 2010; Li, Ezelle et al. 2011). It has been reported that RIG-I acts as a critical pattern-recognition receptor (PRR) for sensing viral RNA pathogen-associated molecular patterns (PAMPs).

Upon RIG-I interacting with RNA substrates, its conformational switch will convert this protein from inactive state to active form, signaling to downstream IFN regulatory factor 3 (IRF3) and NFκB then trigger the transcription and translation of type I interferon (IFN) as well as other inflammatory cytokines to eliminate pathogens(Beutler, Eidenschenk et al. 2007; George, Li et al. 2009).

According to our next generation sequencing (NGS) data, which provide us predicted editing sites and target genes that edited by ADAR1, we found a group of genes are involved in RIG-I-like receptor signaling pathway, suggesting ADAR1 also takes part in this antiviral mechanism. Recently, many researches indicate ADAR1 exert a pro- or an anti-viral function depends on what types of viral infection. Thus, these findings broaden our knowledge that in reality immune response is regulated in a far more complicated mechanism. In this research, we focus on RIG-I and IFN-β promoter stimulator (IPS-1) because it has been reported these two genes are important for sensing viral double stranded RNA, as well as initiating the antiviral immune response. Moreover, IPS-I, also known as mitochondrial antiviral signaling protein (MAVS), has abundant predicted editing sites in our NGS data(Peng, Cheng et al. 2012).

1.3 Janus kinase/signal transducers and activators of transcription (JAK/STAT) pathway

It has been known that RLR signaling pathway can induce the production of type I interferon, which will subsequently activate JAK/STAT pathway in a autocrine or paracrine signaling manner(Content 2009; Wilkins and Gale 2010). Type I IFN, including IFN alpha and IFN beta, are agonists for type I IFN receptor, constituted by interferon (alpha, beta and omega) receptor 1 and 2 (IFNAR1 and IFNAR2). As soon as IFNARs bind to agonists, their specific tyrosine residues will be phosphorylated by JAK, providing docking sites for STAT1 and STAT2. Tyrosine residues of receptor-associated STATs are phosphorylated by JAK, facilitating the formation of STAT1-STAT1 homodimers and STAT1-STAT2 heterodimers(Decker, Muller et al. 2005; Dai, Sayama et al. 2006; de Weerd, Samarajiwa et al. 2007). Both of these dimers will translocate to nucleus, and activate the transcription of target genes by binding to specific promoters. STAT1 homodimers can bind to interferon-gamma-activated sites (GAS) promoter sequence(Chon, Hassanain et al. 1996; Decker, Kovarik et al. 1997). On the other hand, STAT1-STAT2 heterodimers will cooperate with a third protein, IFN regulatory factor 9 (IRF9), forming a complex called IFN-stimulated gene factor 3 (ISGF3) which can bind to IFN-stimulated response element (ISRE) promoter

sequence(Braganca and Civas 1998; Mamane, Heylbroeck et al. 1999; Haller, Kochs et al. 2006). In our NGS data, IFNAR1, IFNAR2, JAK2 and STAT1 are substrates for ADAR1, thus we also bring these genes to our checklist.

1.4 Protein kinase, interferon-inducible double stranded RNA-dependent activator (PRKRA)

PRKRA has been identified as an stress sensor protein, which is up-regulated both in mRNA and protein level after LPS treatment(Yoshida, Okamura et al. 2012). Various manners have been mentioned to activate the activity of this protein, including peroxide, actinomycin D, arsenite treatment and serum starvation(Patel and Sen 1998; Patel, Handy et al. 2000; Li, Peters et al. 2006). PRKRA is known as an activator for eukaryotic translation initiation factor 2-alpha kinase 2 (EIF2AK2), also briefly named as PKR, in the absence of double stranded RNA. After interaction with dsRNA, or activated by PRKRA, the activated PKR can phosphorylate eIF2-alpha, then inhibit the translation and initiate cellular apoptosis(George, Li et al. 2009; Li, Ezelle et al. 2011; Yoshida, Okamura et al. 2012). The biochemical analysis of how PRKRA activates PKR and which residues are important for this mechanism has been described(Peters, Dickerman et al. 2009). Moreover, PKR is thought to be an anti-viral kinase, but it

seems that ADAR1 acts as an pro-viral kinase in some cases by destabilizing the structure of dsRNA(Pfaller, Li et al. 2011).

In our NGS data, PRKRA is also a candidate that will be edited by ADAR1. Besides, it has been reported that PRKRA is an important factor to initiate and maintain the cellular response triggered by RIG-I, suggesting PRKRA has multiple function in cells(Kok, Lui et al. 2011).

2. Materials and methods

2.1 Cell culture

SK-N-SH cells (human neuroblastoma) were grown in Minimum Essential medium (Gibco®) with 10% fetal bovine serum, 0.1 M nonessential amino acids (NEAA) and 1 mM sodium pyruvate (S.P.) at 37°C in humidified incubator containing 5% CO_2. When the cells grew to 90% confluence, one 100-mm dish of SK-N-SH cells were washed by phosphate buffered saline (PBS), then trypsinized by 1 mL 1X trypsin for three minutes at 37°C. The trypsinization is stopped by adding 9 mL growth medium, then cells were sub-cultured to four new 100-mm dishes. Track the passage number of SK-N-SH cells, and maintain the cells in culture up to 20^{th} passage. To freeze cells for the long term storage, trypsinized cells were centrifuged at 500 g for 5 minutes, then removed the supernatant and the cells were resuspended by FBS containing 10% dimethyl sulfoxide (DMSO). After resuspension, the ampoules containing suspending cells were placed in a styrene box, and cooled down gradually from 4°C, -20°C to -80°C. After 16 to 24 hours, the tubes were transferred and stored in liquid nitrogen. Bewared of the exothermic reaction when adding DMSO into FBS. To avoid affecting the efficiency of long term storage, the solution should be prepared in the beginning.

2.1.1 Interferon-gamma treatment

IFN-gamma was purchased from Calbiochem®. Stock solution was kept with 1mM acetic acid and 0.1% bovine serum albumin (BSA) at 10 ng/μL, stored at -20°C, and the final concentration of IFN- gamma was 20 ng/mL in growth medium (Massad, Mutch et al. 1990; Wada, Pai et al. 1997; Tekautz, Zhu et al. 2006). SK-N-SH cells were treated with 20 ng/mL IFN- gamma in 90% confluence for 3 hours.

2.1.2 Polyinosinic: polycytidylic acid (poly(I:C)) treatment

Poly(I:C) was purchased from Sigma-Aldrich (catalog number: P9582). The product was soluble in water, and the concentration of stock is 10 μg/μL in -20°C. To mimic viral infection, SK-N-SH cells were transfected by poly(I:C) with lipofectamine™ 2000 reagent, and the working concentration of poly(I:C) was 2 μg/mL for 20 hours(Chuang, Chuang et al. 2011). One day before transfection, SK-N-SH cells were sub-cultured with 2 mL growth medium in 6-well plates, and the cells would be 90% confluence at the time of transfection. 10 μg poly(I:C) and 5 μL lipofectamine™ 2000 was added in 250 μL pre-warmed OPTI-MEM (Gibco®) and incubated for 5 minutes at room temperature. After the 5 minutes incubation, these two reagents were combined and incubated for 20 minutes at room temperature, then each well was added with 0.5 mL complexes. Medium would be changed after 6 hours.

2.1.3 Actinomycin D treatment.

The stock concentration of actinomycin D (A.D.) was 10 μg/μL in -20°C, and 20 μg/mL was used to block cellular transcription. In addition, 50 ng/mL was used to create a stress condition. Because actinomycin D was hygroscopic and sensitive to light, the stock stored sealed and protected from light and moisture(Wada, Pai et al. 1997; Gupta, Williams et al. 2006).

2.2 siRNA transfection

One day before transfection, SK-N-SH cells were sub-cultured into new 35-mm dishs or 6-well plate. The cell density should be 30-50% confluent as well as grown in 2.5 mL medium without antibiotics at the time of transfection. 100 picomole siRNA and 5 μL lipofectamine™ RNAiMAX were added in 250 μL pre-warmed Opti-MEM respectively, and incubated in room temperature for 5 minutes. Then the diluted RNAi duplex with the diluted Lipofectamine™ RNAiMAX were combined in a new microcentrifuge tube. The mixture was mixed gently and incubated for 20 minutes at room temperature. 500 μL mixture was added into each well and incubate cells in incubator for 48 hours. Medium should be changed after 6 hours. At 48 hours after transfection, total RNA extracts were harvested from individual wells.

2.3 RNA extract and reverse transcription

Growth medium were removed from culture dish by suction, then add 1 mL TRIzol® reagent to the cells directly in each wall of 35-mm dish. The surface area of culture dish was rinsed and the homogenates were pipetted up and down to make sure all cells were lysed. The homogenates were transferred to new RNase-free 1.5 mL microcentrifuge tubes individually, then incubated the samples at room temperature for 5 minutes. 200 μL chloroform was added to each of the homogenates and shook them vigorously by hands for 15 seconds. The samples were incubated at room temperature for 3 minutes, then centrifuged with 1,3000 g for 25 minutes at 4°C. After the centrifugation, samples were separated into a lower phase, an interphase and a colorless upper aqueous phase. The aqueous phase was transferred to new RNase-free 1.5 mL microcentrifuge tubes carefully, mix with 500 μL isopropanol gently until oil-water interface is disrupted. The samples were incubated at room temperature for 10 minutes, then centrifuge them with 1,3000 g for 15 minutes at 4°C. The supernatants were removed, then the pellet was washed through 1 mL 75% ethanol, and the samples were centrifuged with 7500 g for 10 minutes at 4°C. Removed the supernatants, then dried the RNA pellet briefly in hood. Dissolved RNA samples with an adequate amount of RNase-free water.

Measured the concentration of each sample, then added 2 to 5 μg of RNA to 200 μL

RNase free microcentrifuge tubes. After mixing with 1 μL of 10 mM dNTP and 250 ng random hexamer, the mixture was incubated at 65°C for 5 minutes. Then added 4 μL of 5 X transcriptase buffer, 2 μL of 0.1 M dithiothreitol (DTT) and 1 μL of RNase Inhibitor (RNaseOUT™) into the tubes, and incubated the mixture at 37°C for 2 minutes. Finally, add 1 μL moloney murine leukemia virus (MMLV) reverse transcriptase into the tubes, and the mixtures were incubated at 25°C for 10 minutes followed by 50 minutes at 37°C and 15 minutes at 70°C.

2.4 Primer design for end-point polymerase chain reactions and quantification real time polymerase chain reactions

Genomic sequence of each target gene was obtained from UCSC genome browser website. Combine with our next generation sequencing data, amplicon should cover predicted editing sites as many as possible. Each primer contains 20-25 nucleotides, GC content of primers is 50-60% and the range of melting temperature is from 59 to 62°C. The secondary structure, amplicon sequence and melting temperature were confirmed by vector NTI Advance® software and UCSC database.

2.5 End-point polymerase chain reactions

Followd the procedure described in datasheet of Taq DNA polymerase (Roche), 0.5 U polymerase, 10 mM Tris-HCl, 2.5 mM $MgCl_2$, 50 mM KCl, 0.2 mM dNTP mix, 0.6 μM forward primer, 0.6 μM reverse primer and 100-300 ng cDNA were added in 200 μL microcentrifuge tube. Total reaction volume is 25 μL. Samples were vortexed and spun down briefly, then placed samples in a thermal block cycler and used the thermal profiles described in datasheet. The reaction were incubated at 94°C for 4 minutes followed by 30 cycles of 30 seconds at 95°C, 30 seconds at 56-64°C and 45 seconds at 72°C. Following the final cycle of the PCR, the final elongation step was performed at 72°C for 7 minutes. The length of PCR products was confirmed through electrophoresis by 1.2% agarose gel.

2.6 Quantification real time polymerase chain reactions

KAPA™ SYBR® FAST qPCR kit was purchased from KAPABiosystems. Total volume of each reaction was 20 μL, containing 5 picomole forward primer, 5 picomole reverse primer and 20 to 50 ng template DNA. The reaction were incubated at 95°C for 3 minutes followed by 40 cycles of 3 seconds at 95°C and 30 seconds at 60°C. The results were analyzed by Bio-Rad iQ5 software. The PCR products were confirmed through electrophoresis by 1.2% agarose gel.

2.7 Preparation of cell extract

For cell lysates preparation, medium was removed and wells were washed with PBS buffer. After removing PBS buffer, 70 μL whole cell extraction (WCE) (20 mM HEPES pH7.6, 10% glycerol, 0.4 M NaCl, 0.5% Triton-X 100, 1 mM DTT, 5 mM EDTA, 1 mM EGTA, 1 mM PMSF, 1 mg/mL leupeptin and 1 mg/mL pepstatin A) buffer was added into each well of 6-well plate. The cell lysates were collected into new 1.5 mL centrifuge tubes. After centrifugation for 15 minutes in 14000 revolutions per minute (rpm), the supernatants were stored in -80°C.

2.8 Sodium dodecyl sulfate polyacrylamide gel electrophoresis (SDS-PAGE)

Cell lysates were Protein samples were mixed with sample buffer (50 mM Tris (pH6.8), 100 mM DTT, 2% SDS, 0.1% bromophenol blue and 10% glycerol), incubated at 95°C for 10 minutes. Polypeptides were separated according to their molecular weight by polyacrylamide gel with constant voltage of 80 V to 100 V. After the electrophoresis was done, polypeptides were transferred to PVDF membrane through transfer kit with constant current of 180 mA. After transfer was done, PVDF membrane was dunked in 5% fat free milk for 1 hour at 4°C, then added adequate amount of primary antibody (1^{st} Ab) to recognize target proteins. To detect the amount of target proteins expressed in cells with minimized noise signals, PVDF membrane should be

washed by TBST buffer (10 mM Tris (pH8.0), 150 mM NaCl and 0.05% Tween-20), and secondary antibody (2^{nd} Ab) were used to react with the heavy and light chain of 1^{st} Ab. Subsequently, PVDF membrane should be washed again. Because of the conjugation of 2^{nd} Ab with horseradish peroxidase (HRP), which can emit light when acting on enhanced chemiluminescence (ECL), we can detect the expression level of target protein in cells through detecting and analyzing the signal by Bio-Rad Universal Hood II Gel Imager.

2.9 Preparation of polyacrylamide gel

The protocol was described in Molecular Cloning: A Laboratory Manual (4th edition). Separating gel contained 6 to 15% acrylamide mix, 0.375 M Tris (pH8.8), 0.1% SDS, 0.1% ammonium persulfate and 0.08% tetramethylethylenediamine (TEMED). The stacking gel contained 5% acrylamide mix, 0.125 M Tris (pH6.8), 0.1% SDS, 0.1% ammonium persulfate and 0.1% TEMED.

Units: mL	Separating gel				Stacking gel
Gel concentration	8%	10%	12%	15%	5%
ddH_2O	4.6	4.0	3.3	2.3	2.7
30% acrylamide	2.7	3.3	4.0	5.0	0.67
Tris buffer	2.5	2.5	2.5	2.5	0.5
10% SDS	0.1	0.1	0.1	0.1	0.04
10% APS	0.1	0.1	0.1	0.1	0.04
TEMED	0.004	0.004	0.004	0.004	0.004

30% acryamide: 29.2% acrylamide plus 0.8% bis-acrylamide.

Tris buffer for separating gel: 1.5 M Tris (pH8.8)

Tris buffer for stacking gel: 1 M Tris (pH6.8)

2.10 Rapid amplification of 3’ complementary DNA ends (3’ RACE)

RNA samples were harvested through TRIzol® reagent, and the procedures had been mentioned in 2.3. First, RNA samples were treated with alkaline phosphatase to convert RNA with a 5’ monophosphate or a 5’ triphosphate to 5’-hydroxyl ends, thus these RNA would not be modified in following T4 ligation reaction. Second, RNA samples were treated with Tobacco acid pyrophosphatase (TAP) to remove 5’ cap structure of all processed eukaryotic RNA, and these RNA would contain a 5’ monophasphate end. Third, by using T4 RNA ligase, RNAs contained 5’ monophasphate end would be linked to an unique oligomer, which would be specifically recognized by the kit-offering primer. Finally, through using kit-offering primer and our own primers, amplicon was amplified in a plus strand specific way. More details were mentioned in ExactSTART™ Eukaryotic mRNA 5’- & 3'-RACE Kit.

2.11 Preparation of DNA constructs

TOPO TA Cloning® (invitrogen) reagent was stored at -20°C. Insert fragments were amplified through end-point PCR as mentioned earlier. 2 μL of fresh PCR products were mixed with 0.5 μL TOPO TA Cloning® reagent and 0.5μL salt solution (1.2 M NaCl and 0.06 M $MgCl_2$). The mixture was incubated at 22°C for 10 minutes.

2.12 Preparation of agar plate and plasmid transformation

5 g tryptone, 2.5 g NaCl, 2.5 g yeast extract and 7.5 g agar were added into 500 mL distilled water in a clean 1L flask. Covered the flask with aluminum foil and autoclaved for 20 minutes. When the agar had been autoclaved, allowed it to be cool until the bottle can be held with bare hands for at least 10 seconds. 500 μL ampicillin (1 mg per mL) was added in the flask, mixed gently and poured out carefully into sterile plastic petri dishes. After agar solidification, stored the plates at 4°C.

50 ng plasmid was added into 1.5 mL microcentrifuge tubes containing 20 μL DH5α competent cells, then put tubes on ice for 20 minutes. The cells were heat shocked at 42°C in water bath for 90 seconds then put on ice to cool down immediately for 3 minutes. 500 μL LB broth was added in tubes, then incubated on shaker at 37°C for 1 hour. After centrifugation at 3,000 rpm for 1 minute, pellet was resuspended in 100μL LB broth and spread on LB plates. The plates were incubated at 37°C for 14 to 16 hour, then stored at 4°C.

3. Results

Part I. Target genes edited by ADAR1 and their RNA expression level after ADAR1 knockdown.

3.1 Editing sites of genes involved in RLR and JAK/STAT signaling pathway predicted in our NGS data were confirmed by Sanger sequencing.

According to our NGS data, IFNAR1, IFNAR2, STAT1, JAK2 and IFI27L1, which involved in Jak/STAT signaling pathway, and RIG-I as well as MAVS, which take part in RLR pathway, were editing substrates for ADAR1 (figure 1A, 1C, 1E, 1G, 1I, 1K and 1M). To further confirm the editing events, the fragments containing predicted editing sites were amplified through specific primers in SK-N-SH cells, rather than YH cells, for the reason that ADAR1 was abundant in neuron cells; furthermore, RLR and JAK/STAT signaling pathway was inducible in neurons, thus SK-N-SH was suitable for our researches in future. The sequencing data of IFNAR1, IFNAR2, IFI27L1, RIG-I and MAVS showed that the adenine to inosine events were eliminated or at least reduced (figure 1B, 1D, 1F, 1H and 1J). Many editing sites predicted by our NGS data had been confirmed. Moreover, many additional sites that not identified in our NGS data are also modified by ADAR1. However, no editing events were observed in STAT1 and JAK2 (figure 1L and 1N). This might be because the thresholds of the filter criteria were not be comprehensive enough to rule out some fault editing sites predicted in our NGS data,

or these editing events occurred in a cell-specific way.

3.2 Expression level of mRNA and edited fragment of most target genes were not altered after ADAR1 knockdown.

It had been reported that ADAR1 was associated with various RNA processing steps;fFor this reason, we test if the mRNA expression level of each target genes was altered after ADAR1 knockdown by real-time PCR. Based on our results, ADAR1 knockdown efficiency was about eighty percent (figure 2B) compared to the internal control, elongation factor 1 alpha (eEF1α), (figure 2A); nevertheless, no significant difference of mRNA expression level had been found in IFNAR1, IFNAR2 and MAVS (figure 2C, 2D and 2F). Interestingly, it seemed that mRNA of IFI27L1 (figure 2E) was slightly increased. Moreover, the RNA expression level of edited fragments, either in 3'UTR or introns, of these genes were increased after ADAR1 knockdown (figure 3). Based on these results, we concluded that the mRNA expression level of most of the target genes was not changed after the A to I editing, even the editing events of these genes were obvious.

3.3 RNA stability of IFNAR1 IFNAR2 and IFI27L1 was not changed after ADAR1 knockdown.

For the reason that mRNA expression level of IFNAR1 and IFNAR2 was not altered after ADAR1 knockdown, we next wondered if ADAR1 might have ability to affect RNA stability of these genes. At first, we measured the RNA expression level of target genes for 48 hours after siRNA transfection, but RNA stability of these genes remained stable and we cannot observe apparently differences. Thus we were curious about the fact that if the differences would be more obvious under the condition that their RNA expression had been induced. To activate the IFN-signaling pathway, we used IFN-gamma to treat with SK-N-SH cells. The downstream markers for IFN-gamma treatment we used were interferon regulatory factor 1 (IRF-1) and major histocompatibility complex, class II, DR alpha (HLA-DRα)(Patterson, Thomis et al. 1995). After IFN-gamma treatment, mRNA expression level of IRF-1 and HLA-DRαIt were increased significantly (figure 4A-4C), suggesting this signaling pathway was inducible in SK-N-SH cells. Besides, it had been reported that IFN-gamma might up-regulate mRNA expression level of ADAR1, type I interferon and IFN receptors, including IFNAR1 and IFNAR2(Mizukoshi, Kaneko et al. 1999), thus we also detected the mRNA expression of these genes after IFN-gamma treatment. Consistent with previous reports, in our results, mRNA of IFNAR1 and IFNAR2 are twofold increased

(figure 4D, 4E and 4F), suggesting JAK/STAT signaling pathway was inducible.

In this experiment, early growth response 1 (EGR-1) as well as v-myc myelocytomatosis viral related oncogene, neuroblastoma (N-myc) were chosen as our positive control(Wada, Pai et al. 1997; Giraldo, Barrett et al. 2012), and the internal control was eEF1α, for its mRNA expression level remains constant (figure 5A). The ADAR1 knockdown efficiency was about 80%, consistent with earlier results (figure 5B). It matched our expectation that and mRNA expression of N-Myc was decreased gradually with the passing time (figure 5C). As for IFNAR1, IFNAR2 and IFI27L1, their RNA stability were stable even 180 minutes after actinomycin D treatment (figure 5D-5F). These results suggested that ADAR1 knockdown was not associated with regulation of RNA stability of IFNAR1, IFNAR2 and IFI27L1. Interestingly, it had been mentioned IFI27L1 mRNA was increased after ADAR1 knockdown, and this increase could be detected for 3 hour after actinomycin D treatment (figure 5G).

Part II. The antisense transcript overlapping with 3' UTR of PRKRA transcript.

3.4 mRNA and protein expression level of PRKRA was reduced after ADAR1 knockdown.

In our NGS data, PRKRA transcript was noticeable because it contained A to I editing sites at its 5' region and U to C editing sites near its 3' region, suggesting there

was an antisense transcript overlapping with 3' region of PRKRA (figure 8). We tried to check the A to I editing events of PRKRA. Because most of the sequences surrounded by predicted editing sites contained abundant repeat sequences, making it difficult to find suitable primers, not all the editing sites of PRKRA were confirmed. For this reason, we measured the expression of mRNA and protein of PRKRA at first. Interestingly, we observed a statistical significant decrease of PRKRA in both mRNA and protein expression level after ADAR1 knockdown (figure 6A, 6B). On the other hand, part of the editing sites were confirmed (figure 7A, 7B). Though the background noises were not fully abolished, the T to C editing events were confirmed and the signals were distinct. Thus we suggested that there was an antisense transcript overlapping with PRKRA, and this antisense transcript was also a substrate edited by ADAR1.

3.5 A predicted antisense was overlapped with 3' UTR of PRKRA by combining the bioinformation from University of California Santa Cruz (UCSC) and Generic Genome Browser (GBrowser) database.

To confirm the existence of the predicted antisense transcript, the bioinformation from two database, UCSC and GBrowser, were taken for our reference. UCSC supplied the sequence and position of known transcripts; in the other hand, GBrowser provided

the transcripts expression profile of whole human genome. After counting the number of reads per five hundreds of nucleotides, the transcripts expression profile showed peaks in between 179,004,395 to 179,024,110 of minus strand of chromosome 2 (figure 8B), consistent with the location of PRKRA (figure 8, dotted line). Expectedly, signal peaks were also detected between approximately 178,998,000 to 179,013,000 on plus strand of chromosome 2, showing a transcript overlapping with 3' UTR of PRKRA transcript. These data predicted the existence and rough region where the antisense transcripts supposed to be located.

3.6 The existence and rough location of the antisense transcript was investigated by 3' RACE.

To further confirm the existence of the antisense transcript, we used 3' RACE combined with primers specific to plus strand to amplify the partial region among the antisense transcript (figure 9A). Subsequently, the 3' RACE products were utilized as template and detected by primer 1 to 6 through end-point PCR (figure 9B). All the primers, except for primer 1, which located in 5' region of PRKRA transcript where was separated with the predicted antisense transcript, were located in the overlapped region. As expected, there was no PCR products of primer 1 (figure 9C); on the other hand, signals of other primers, including primer 2 to primer 6 were observable (figure 9C). In

addition, we designed three pairs of primers which were situated at downstream of PRKRA transcript to estimate the position of 5' end of the antisense transcript (figure 10A). The results demonstrated that when whole genome transcripts were used as template, signals of these three primers were detectable in HUVEC (human umbilical vein endothelial cells, EC) (figure 10B). When the 3' RACE products were applied as template, signals of primer 1 and primer 2 were still obvious; however, no signal of primer 3 was detectable (figure 10B). Our results proved the existence of the antisense transcript, which was estimated about 12.5 kb based on our results. It remained unclear if this antisense transcript was produced from a larger transcript which processing splicing. For this reason, we used SFmap database to predict the splicing factor binding sites(Akerman, David-Eden et al. 2009; Paz, Akerman et al. 2010), trying to figure out whether there were predicted splicing sites near the antisense transcript (figure 11). The results showed there were abundant splicing factor binding sites in middle of the antisense transcript, and we hypothesized that this transcript might has been spliced. Nevertheless, it needed more experimental data to elucidate these puzzles.

3.7 RNA stability of the antisense transcript was improved after ADAR1 knockdown.

Subsequently, we wondered if ADAR1 affected RNA stability of PRKRA and the antisense transcript. Consistent with previous data, mRNA of PRKRA was decreased after ADAR1 knockdown, but its RNA stability remained stable even 3 hours after actinomycin D treatment (figure 12A). Surprisingly, the half-life of the antisense transcript was prolonged after ADAR1 knockdown, from 30 minutes to 75 minutes (figure 12B). These results indicated that ADAR1 might has the ability to regulate RNA stability of the antisense transcript. Moreover, our previous data suggested ADAR1 knockdown will cause decreased protein expression level of PRKRA; therefore, we wondered if the antisense transcript had ability to interfere PRKRA at RNA or protein level, and ADAR1 had function to enhance the activity of the antisense transcript.

3.8 PKR phosphorylation could be reduced after ADAR1 knockdown under stress condition.

It has been known that PRKRA was a stress sensor, and it could catalyze the phosphorylation of PKR to pPKR, which exert the catalytic activity. Subsequently, pPKR could turn on the downstream signaling pathway. To understand whether ADAR1 knockdown would cause not only reduced PRKRA at protein level, but also interfered

cells to sense stress stimulation, we utilized serum free medium plus actinomycin D to induce the stress response, and detectd the PKR and pPKR protein expression level by Western blotting (figure 13). It seemed that after the stress stimulation, amount of total PKR and pPKR was raised either in control or ADAR1 knockdown condition. Moreover, the ratio of pPKR to PKR was slightly decreased after ADAR1 knockdown (figure 14). Our results suggest ADAR1 was involved in sensing stress stimulation, but this system we used was too complicated to answer these questions. For this reason, more data were required to get the details.

Part III.

3.9 mRNA expression of IFNB1, PKR and STAT1 induced by poly(I:C) was not altered after ADAR1 knockdown.

It had been reported ADAR1 acted both pro-viral and anti-viral roles, depending on different virus infection. To elucidate the complexity of the regulatory machinery, in the beginning, we used poly(I:C) to mimic RNA virus infection, then used qPCR to measure the mRNA expression level of genes downstream of RLR pathway, including PKR, STAT1 and IFNB1, to understand if ADAR1 had an effect on the induction of these genes. In this experiment, we knockdown ADAR1 by siRNA transfection for 24 hours, followed by poly(I:C) transfection for 18 and 24 hours. Our results indicated that

the mRNA expression level of PKR, STAT1 and IFNB1 were dramatically increased after poly(I:C) transfection (figure 15), suggesting RLR pathway was inducible in SK-N-SH cells. After poly(I:C) treatment for 24 hours, mRNA expression level of IFNB1, PKR and STAT1 were not altered after ADAR1 knockdown (figure 16B, 16C, 16D and 16E). These results suggested the RLR signaling pathway induced by poly(I:C) was not affected by ADAR1, at least in mRNA production of IFNB1, PKR and STAT1.

3.10 Antisense transcript was up-regulated after poly(I:C) treatment.

Interestingly, after poly(I:C) treatment, the expression level of antisense transcript was increased about fivefold (figure 17B). In addition, the mRNA expression level of PRKRA was statistically significantly reduced (figure 17A), suggesting the antisense transcript may regulate PRKRA at RNA level. Subsequently, we want to know whether this increase of the antisense transcript affects PRKRA in protein level. Intriguingly, after poly(I:C) treatment for 2 to 24 hours, protein level of PRKRA was reduced gradually (figure 18). It had been reported that PRKRA was an activator for PKR, thus we wondered if lower phosphorylated PKR would be detected in this condition. Surprisingly, although the ratio of phospho-PKR/PKR was progressively increased, both phospho-PKR and PKR were reduced in protein level (figure 18).

4. Discussion

4.1 Numerous genes involved in immune signaling pathways were edited by ADAR1.

In this research, many editing sites were confirmed by Sanger sequencing; moreover, most of the editing events were abolished after ADAR1 knockdown, suggesting ADAR1 played a major role in triggering the editing on these genes. Although it seemed that the mRNA expression of MAVS, IFNAR1 and IFNAR2 remained equal, IFI27L1, which was induced through type I interferon was slightly increased. It had been reported that transcripts of interferon-stimulated genes (ISGs) were up-regulated after ADAR1 knockdown(Hartner, Walkley et al. 2009), the details of the phenomenon were still not clear. Thus, we suggested that mRNA increase of IFI27L1 may be because ADAR1 directly facilitated the RNA processing and maturation by interacting with their transcripts, or the signaling to induce the transcription of IFI27L1 was enhanced by ADAR1 through interacting with the genes involved in the signaling pathway(Nie, Ding et al. 2005; Gommans and Maas 2008). IFI27L1 was a novel protein first described in 2005, and its cellular function remained unclear(Folgueira, Carraro et al. 2005). On the other hand, the homologous protein, interferon, alpha-inducible protein 27 (IFI27)(Martensen and Justesen 2004), was more discussed as well as was considered as a cancer marker for certain epithelial

cancers(Suomela, Cao et al. 2004; Cheriyath, Leaman et al. 2011), and was involved in cellular apoptosis(Rosebeck and Leaman 2008). Moreover, it had been reported both ADAR1 knockout mice and MEF cells were prone to apoptosis(Wang, Miyakoda et al. 2004). Although the relationship between IFI27L1 and ADAR1 had not been investigated so far, it was possible that ADAR1 was involved in certain cancers and apoptosis by interacting with IFI27L1.

4.2 PRKRA may be regulated by the antisense transcript which were edited by ADAR1.

In our NGS data, the editing events could be distinguished through a strand specific manner. Thus, it was possible the T to C editing on RNA transcript transcripted from plus strand was actually an A to I editing on RNA transcript transcripted from minus strand, and vise versa. For this reason, it was possible that our NGS data could provide us the information to predict the existence of antisense transcripts. Based on this feature of NGS, we found an antisense transcript overlapping with PRKRA, and our results suggested its RNA stability was prolonged after ADAR1 knockdown. Some researches indicated that antisense transcripts had the ability to regulate RNA expression by interfering the transcription of target genes(Donaldson and Saville 2012). Although antisense transcripts had become a hot issue recently, the understanding of their

orientation and biological function remained ambiguous(Ho, Tsai et al. 2012). In this study, we found the antisense transcript, which overlapped with 3' UTR of PRKRA transcript, was inducible after poly(I:C) treatment; in more details, the ratio of the antisense transcript to PRKRA was up-regulated from about 1/10 to 1/2. Moreover, mRNA of PRKRA was statistically significantly decreased after poly(I:C) treatment. These findings hypothesized a PRKRA regulation network which was made up by ADAR1 and the antisense transcript. Furthermore, the founding of antisense transcripts participating in this pathway, suggested that there was a more complicated regulatory process beyond the mechanism. Moreover, these findings extended the cellular functions of ADAR1 that interacting with antisense transcripts which played some biological function to specifically regulate the RNA expression; that was to say these antisense transcripts were regulated by ADAR1. Furthermore, based on the comparative analysis, some researches indicated the substrates edited by ADAR1 were evolved from transposon elements, repeat sequences and intermolecular interaction between sense and antisense transcripts(Jin, Zhang et al. 2009). Therefore, it was probable that ADAR1 involved in more cellular events which has been reported by interacting with the antisense transcripts.

4.3 ADAR1 was associated with virus infection.

Because ADAR1 was an IFN-inducible gene, it was reasonable to suggest ADAR1 took part in immune systems. Recently, many researches indicated ADAR1 was indeed associated with the regulation of virus infection; surprisingly, many findings indicated that ADAR1 often showed pro-viral activity(Samuel 2011). For instance, it had been reported that ADAR1 assisted the production of delta antigen, large form (HDAg-L) which was encoded by hepatitis D virus (HDV), and this protein was necessary for packaging of the viral genome and HDV particles formation(Taylor 2003; Casey 2006). In contrast, it had been reported that after the measles virus (MV) infection in ADAR1p150 null mouse embryo fibroblast (MEF), enhanced syncytium formation and virus-induced cytotoxicity would be observed (Toth, Li et al. 2009). In addition, compared to wild type MEF, ADAR1p150 null MEF also showed extended virus-induced cytotoxicity after influenza A virus infection(Ward, George et al. 2011). It had been reported that MS could activate RLR signaling pathway by interacting with MAVS(Randall and Goodbourn 2008; McAllister, Toth et al. 2010), then induced the production of interferon beta. Moreover, PRKRA was required for triggering RLR signaling pathway by interacting with RIG-I protein(Kok, Lui et al. 2011). In our results, after poly(I:C) transfection, the mRNA expression of interferon beta was up-regulated, but this induction was not changed after ADAR1 knockdown in SK-N-SH

cells. Though using poly(I:C) transfection to mimic the virus infection was under debate, we still anticipated we could decipher some questions by this system.

4.4 Our NGS data provides various target genes which were worth to study.

It had been reported that the regulation of RNA stability was a manner to regulate gene expression(Wu and Brewer 2012), and the interaction between AU-rich elements (AREs), which were usually located in 3' UTR, and specific trans-acting factors played important roles in this process(Meisner, Hackermuller et al. 2004). There were five groups of AREs has been identified so far, and it had been proposed different AREs might increase or decrease the stability of mRNA. Moreover, in our NGS database, many predicted editing sites were positioned in 3' UTR. Therefore, ADAR1 might have function to regulate RNA stability by editing the sequence of ARE or competing with trans-acting factors. Besides, according to the information from AU-RICH ELEMENT-CONTAINING mRNA DATABASE (ARED)(Bakheet, Frevel et al. 2001; Bakheet, Williams et al. 2006), it suggested 3' UTR of IFNAR1 contained an ARE, which belonged to group V cluster. Although the mRNA stability of IFNAR1 remained equal after ADAR1 knockdown in our results, the relationship between ADAR1 and AREs was still worth to study, because there were various interesting candidates in our list not discussed in this research.

Various target genes were predicted to be edited by ADAR1 according to our NGS data. In the beginning, we used the database for annotation, visualization and integrated discovery (DAVID) to classify these genes to the signaling pathway they belonged to, trying to figure out which pathways were most likely under the regulation of ADAR1. Based on the results we searched out from DAVID, five immune-associated pathways were concerned, including RLR signaling pathway, JAK/STAT signaling pathway, TLR signaling pathway, chemokine signaling pathway as well as IFN-IFN receptor interaction. In this research, we focused on RLR and JAK/STAT signaling pathway as our target, not only because the correlation of these two pathways but also the other pathways were much implicated in various cellular signaling and events, including MAPK signaling pathway, proteolysis, regulation of actin cytoskeleton and so on, making it harder for us to decipher and conclude the observations. Therefore, details of how ADAR1 regulating immune signaling was still not clear, and many questions remained to be solved.

5. References

Akerman, M., H. David-Eden, et al. (2009). "A computational approach for genome-wide mapping of splicing factor binding sites." Genome Biol **10**(3): R30.

Bakheet, T., M. Frevel, et al. (2001). "ARED: human AU-rich element-containing mRNA database reveals an unexpectedly diverse functional repertoire of encoded proteins." Nucleic Acids Res **29**(1): 246-254.

Bakheet, T., B. R. Williams, et al. (2006). "ARED 3.0: the large and diverse AU-rich transcriptome." Nucleic Acids Res **34**(Database issue): D111-114.

Beutler, B., C. Eidenschenk, et al. (2007). "Genetic analysis of resistance to viral infection." Nat Rev Immunol **7**(10): 753-766.

Braganca, J. and A. Civas (1998). "Type I interferon gene expression: differential expression of IFN-A genes induced by viruses and double-stranded RNA." Biochimie **80**(8-9): 673-687.

Casey, J. L. (2006). "RNA editing in hepatitis delta virus." Curr Top Microbiol Immunol **307**: 67-89.

Cheriyath, V., D. W. Leaman, et al. (2011). "Emerging roles of FAM14 family members (G1P3/ISG 6-16 and ISG12/IFI27) in innate immunity and cancer." J Interferon Cytokine Res **31**(1): 173-181.

Chon, S. Y., H. H. Hassanain, et al. (1996). "Cooperative role of interferon regulatory factor 1 and p91 (STAT1) response elements in interferon-gamma-inducible expression of human indoleamine 2,3-dioxygenase gene." J Biol Chem **271**(29): 17247-17252.

Chuang, J. H., H. C. Chuang, et al. (2011). "Differential toll-like receptor 3 (TLR3) expression and apoptotic response to TLR3 agonist in human neuroblastoma cells." J Biomed Sci **18**: 65.

Content, J. (2009). "Mechanisms of induction and action of interferons." Verh K Acad Geneeskd Belg **71**(1-2): 51-71.

Dai, X., K. Sayama, et al. (2006). "SOCS1-negative feedback of STAT1 activation is a key pathway in the dsRNA-induced innate immune response of human keratinocytes." J Invest Dermatol **126**(7): 1574-1581.

de Weerd, N. A., S. A. Samarajiwa, et al. (2007). "Type I interferon receptors: biochemistry and biological functions." J Biol Chem **282**(28): 20053-20057.

Decker, T., P. Kovarik, et al. (1997). "GAS elements: a few nucleotides with a major impact on cytokine-induced gene expression." J Interferon Cytokine Res **17**(3): 121-134.

Decker, T., M. Muller, et al. (2005). "The yin and yang of type I interferon activity in bacterial infection." Nat Rev Immunol **5**(9): 675-687.

Donaldson, M. E. and B. J. Saville (2012). "Natural antisense transcripts in Fungi." Mol Microbiol.

Folgueira, M. A., D. M. Carraro, et al. (2005). "Gene expression profile associated with response to doxorubicin-based therapy in breast cancer." Clin Cancer Res **11**(20): 7434-7443.

Garcia-Sastre, A. (2011). "Induction and evasion of type I interferon responses by influenza viruses." Virus Res **162**(1-2): 12-18.

George, C. X., Z. Li, et al. (2009). "Tipping the balance: antagonism of PKR kinase and ADAR1 deaminase functions by virus gene products." J Interferon Cytokine Res **29**(9): 477-487.

Giraldo, A., O. P. Barrett, et al. (2012). "Feedback regulation by Atf3 in the endothelin-1-responsive transcriptome of cardiomyocytes: Egr1 is a principal Atf3 target." Biochem J **444**(2): 343-355.

Gommans, W. M. and S. Maas (2008). "Characterization of ADAR1-mediated modulation of gene expression." Biochem Biophys Res Commun **377**(1): 170-175.

Gupta, A., B. R. Williams, et al. (2006). "Cellular retinoic acid-binding protein II is a direct transcriptional target of MycN in neuroblastoma." Cancer Res **66**(16): 8100-8108.

Haller, O., G. Kochs, et al. (2006). "The interferon response circuit: induction and suppression by pathogenic viruses." Virology **344**(1): 119-130.

Hartner, J. C., C. R. Walkley, et al. (2009). "ADAR1 is essential for the maintenance of hematopoiesis and suppression of interferon signaling." Nat Immunol **10**(1): 109-115.

Ho, M. R., K. W. Tsai, et al. (2012). "A Unified Framework of Overlapping Genes: Towards the Origination and Endogenic Regulation." Genomics.

Jantsch, M. F. (2010). "Reaching complexity through RNA editing." RNA Biol **7**(2): 191.

Jin, Y., W. Zhang, et al. (2009). "Origins and evolution of ADAR-mediated RNA editing." IUBMB Life **61**(6): 572-578.

Kok, K. H., P. Y. Lui, et al. (2011). "The double-stranded RNA-binding protein PACT functions as a cellular activator of RIG-I to facilitate innate antiviral response." Cell Host Microbe **9**(4): 299-309.

Li, S., G. A. Peters, et al. (2006). "Molecular basis for PKR activation by PACT or dsRNA." Proc Natl Acad Sci U S A **103**(26): 10005-10010.

Li, X. L., H. J. Ezelle, et al. (2011). "A central role for RNA in the induction and biological activities of type 1 interferons." Wiley Interdiscip Rev RNA **2**(1): 58-78.

Li, Z., K. M. Okonski, et al. (2012). "Adenosine deaminase acting on RNA 1 (ADAR1) suppresses the induction of interferon by measles virus." J Virol **86**(7):

3787-3794.

Mamane, Y., C. Heylbroeck, et al. (1999). "Interferon regulatory factors: the next generation." Gene **237**(1): 1-14.

Martensen, P. M. and J. Justesen (2004). "Small ISGs coming forward." J Interferon Cytokine Res **24**(1): 1-19.

Massad, L. S., D. G. Mutch, et al. (1990). "Expression of a resistance mechanism in ovarian and cervical carcinoma cells prevents their lysis by gamma-interferon." Cancer Res **50**(16): 4923-4928.

McAllister, C. S., A. M. Toth, et al. (2010). "Mechanisms of protein kinase PKR-mediated amplification of beta interferon induction by C protein-deficient measles virus." J Virol **84**(1): 380-386.

Meisner, N. C., J. Hackermuller, et al. (2004). "mRNA openers and closers: modulating AU-rich element-controlled mRNA stability by a molecular switch in mRNA secondary structure." Chembiochem **5**(10): 1432-1447.

Melcher, T., S. Maas, et al. (1996). "RED2, a brain-specific member of the RNA-specific adenosine deaminase family." J Biol Chem **271**(50): 31795-31798.

Melcher, T., S. Maas, et al. (1996). "A mammalian RNA editing enzyme." Nature **379**(6564): 460-464.

Mizukoshi, E., S. Kaneko, et al. (1999). "Upregulation of type I interferon receptor by IFN-gamma." J Interferon Cytokine Res **19**(9): 1019-1023.

Nie, Y., L. Ding, et al. (2005). "ADAR1 interacts with NF90 through double-stranded RNA and regulates NF90-mediated gene expression independently of RNA editing." Mol Cell Biol **25**(16): 6956-6963.

Nishikura, K. (2010). "Functions and regulation of RNA editing by ADAR deaminases." Annu Rev Biochem **79**: 321-349.

Orlandi, C., A. Barbon, et al. (2012). "Activity regulation of adenosine deaminases acting on RNA (ADARs)." Mol Neurobiol **45**(1): 61-75.

Patel, C. V., I. Handy, et al. (2000). "PACT, a stress-modulated cellular activator of interferon-induced double-stranded RNA-activated protein kinase, PKR." J Biol Chem **275**(48): 37993-37998.

Patel, R. C. and G. C. Sen (1998). "PACT, a protein activator of the interferon-induced protein kinase, PKR." EMBO J **17**(15): 4379-4390.

Patterson, J. B. and C. E. Samuel (1995). "Expression and regulation by interferon of a double-stranded-RNA-specific adenosine deaminase from human cells: evidence for two forms of the deaminase." Mol Cell Biol **15**(10): 5376-5388.

Patterson, J. B., D. C. Thomis, et al. (1995). "Mechanism of interferon action: double-stranded RNA-specific adenosine deaminase from human cells is inducible by alpha and gamma interferons." Virology **210**(2): 508-511.

Paz, I., M. Akerman, et al. (2010). "SFmap: a web server for motif analysis and prediction of splicing factor binding sites." Nucleic Acids Res **38**(Web Server issue): W281-285.

Peng, Z., Y. Cheng, et al. (2012). "Comprehensive analysis of RNA-Seq data reveals extensive RNA editing in a human transcriptome." Nat Biotechnol **30**(3): 253-260.

Peters, G. A., B. Dickerman, et al. (2009). "Biochemical analysis of PKR activation by PACT." Biochemistry **48**(31): 7441-7447.

Pfaller, C. K., Z. Li, et al. (2011). "Protein kinase PKR and RNA adenosine deaminase ADAR1: new roles for old players as modulators of the interferon response." Curr Opin Immunol **23**(5): 573-582.

Randall, R. E. and S. Goodbourn (2008). "Interferons and viruses: an interplay between induction, signalling, antiviral responses and virus countermeasures." J Gen Virol **89**(Pt 1): 1-47.

Rosebeck, S. and D. W. Leaman (2008). "Mitochondrial localization and pro-apoptotic effects of the interferon-inducible protein ISG12a." Apoptosis **13**(4): 562-572.

Samuel, C. E. (2011). "Adenosine deaminases acting on RNA (ADARs) are both antiviral and proviral." Virology **411**(2): 180-193.

Suomela, S., L. Cao, et al. (2004). "Interferon alpha-inducible protein 27 (IFI27) is upregulated in psoriatic skin and certain epithelial cancers." J Invest Dermatol **122**(3): 717-721.

Taylor, J. M. (2003). "Replication of human hepatitis delta virus: recent developments." Trends Microbiol **11**(4): 185-190.

Tekautz, T. M., K. Zhu, et al. (2006). "Evaluation of IFN-gamma effects on apoptosis and gene expression in neuroblastoma--preclinical studies." Biochim Biophys Acta **1763**(10): 1000-1010.

Toth, A. M., Z. Li, et al. (2009). "RNA-specific adenosine deaminase ADAR1 suppresses measles virus-induced apoptosis and activation of protein kinase PKR." J Biol Chem **284**(43): 29350-29356.

Wada, R. K., D. S. Pai, et al. (1997). "Interferon-gamma and retinoic acid down-regulate N-myc in neuroblastoma through complementary mechanisms of action." Cancer Lett **121**(2): 181-188.

Wahlstedt, H. and M. Ohman (2011). "Site-selective versus promiscuous A-to-I editing." Wiley Interdiscip Rev RNA **2**(6): 761-771.

Wang, Q., M. Miyakoda, et al. (2004). "Stress-induced apoptosis associated with null mutation of ADAR1 RNA editing deaminase gene." J Biol Chem **279**(6): 4952-4961.

Ward, S. V., C. X. George, et al. (2011). "RNA editing enzyme adenosine deaminase is a

restriction factor for controlling measles virus replication that also is required for embryogenesis." Proc Natl Acad Sci U S A **108**(1): 331-336.

Ward, S. V., D. Markle, et al. (2002). "The promoter-proximal KCS element of the PKR kinase gene enhances transcription irrespective of orientation and position relative to the ISRE element and is functionally distinct from the KCS-like element of the ADAR deaminase Promoter." J Interferon Cytokine Res **22**(8): 891-898.

Wilkins, C. and M. Gale, Jr. (2010). "Recognition of viruses by cytoplasmic sensors." Curr Opin Immunol **22**(1): 41-47.

Wu, X. and G. Brewer (2012). "The regulation of mRNA stability in mammalian cells: 2.0." Gene **500**(1): 10-21.

Yoshida, K., H. Okamura, et al. (2012). "Interaction between PKR and PACT mediated by LPS-inducible NF-kappaB in human gingival cells." J Cell Biochem **113**(1): 165-173.

Zinshteyn, B. and K. Nishikura (2009). "Adenosine-to-inosine RNA editing." Wiley Interdiscip Rev Syst Biol Med **1**(2): 202-209.

6. Figures

A

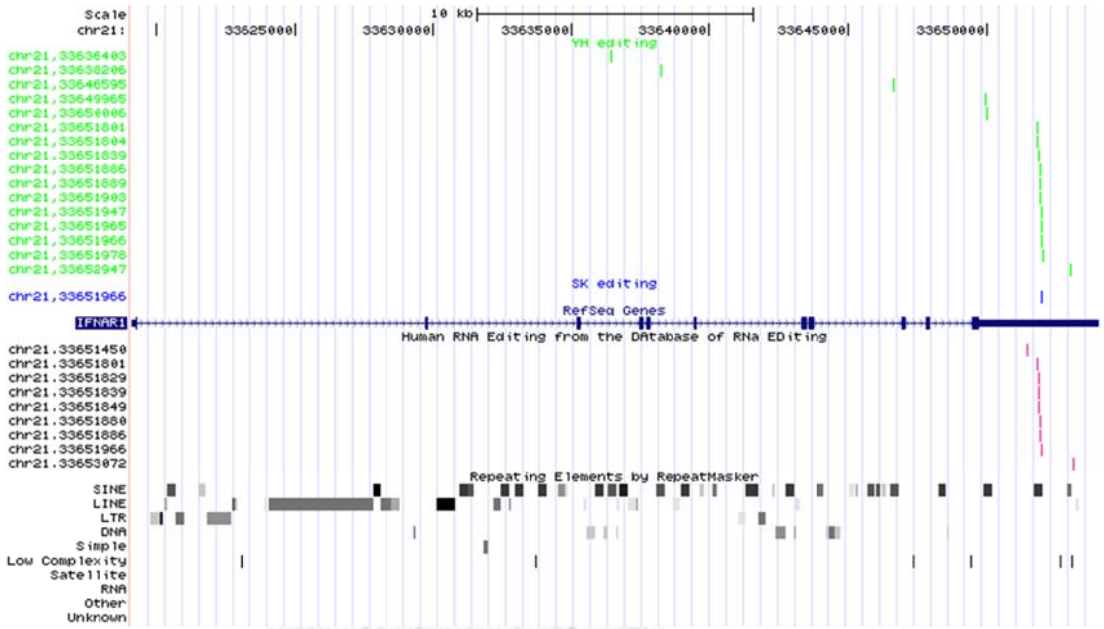
Scale
chr21:
10 kb
33625000
33630000
33635000
33640000
33645000
33650000
YH editing
chr21,33636403
chr21,33638206
chr21,33646595
chr21,33649965
chr21,33650006
chr21,33651801
chr21,33651804
chr21,33651839
chr21,33651886
chr21,33651889
chr21,33651903
chr21,33651947
chr21,33651965
chr21,33651966
chr21,33651978
chr21,33652947
SK editing
chr21,33651966
RefSeq Genes
IFNAR1
Human RNA Editing from the DAtabase of RNA EDiting
chr21.33651450
chr21.33651801
chr21.33651829
chr21.33651839
chr21.33651849
chr21.33651880
chr21.33651886
chr21.33651966
chr21.33653072
Repeating Elements by RepeatMasker
SINE
LINE
LTR
DNA
Simple
Low Complexity
Satellite
RNA
Other
Unknown

B

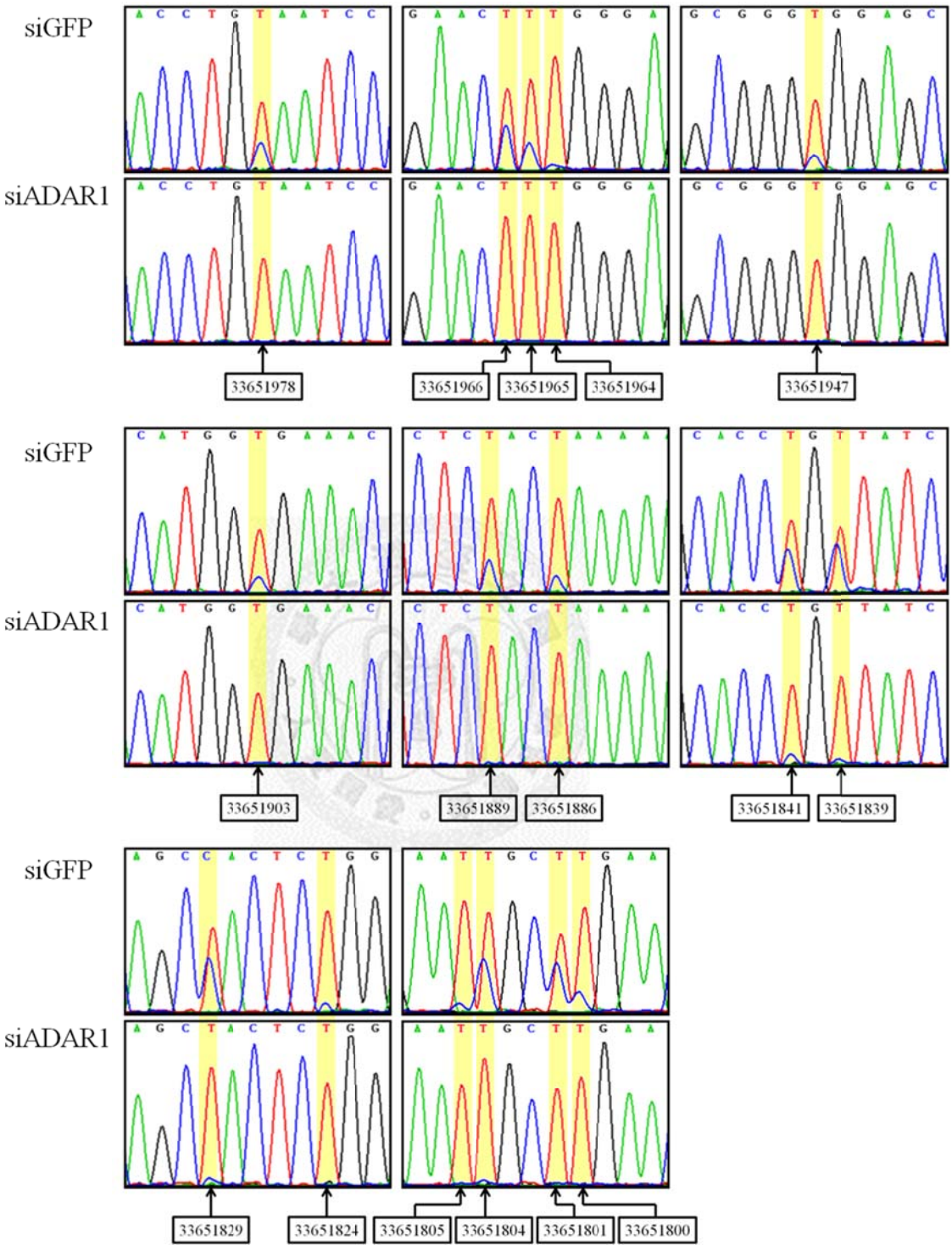
siGFP
siADAR1
33651978
33651966
33651965
33651964
33651947
siGFP
siADAR1
33651903
33651889
33651886
33651841
33651839
siGFP
siADAR1
33651829
33651824
33651805
33651804
33651801
33651800

C

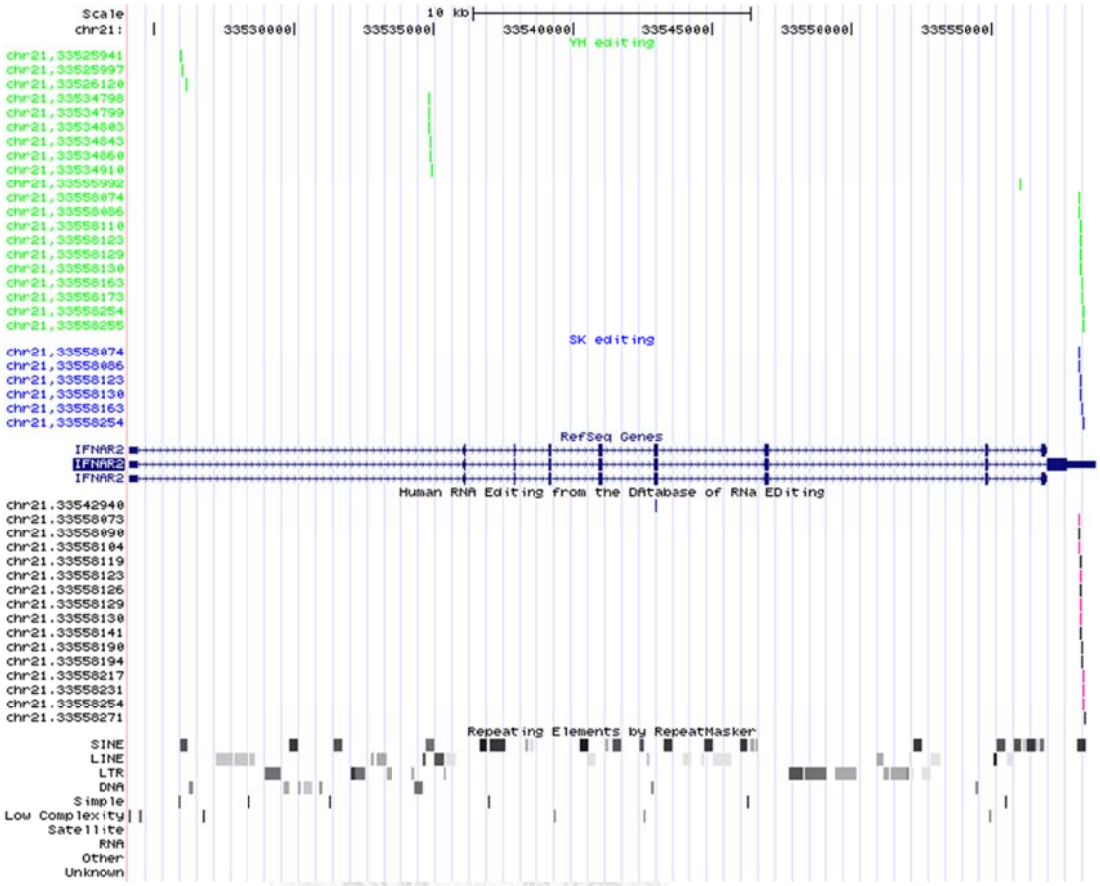
Scale
chr21:
10 kb
33530000
33535000
33540000
33545000
33550000
33555000
YH editing
chr21,33525941
chr21,33525997
chr21,33526120
chr21,33534798
chr21,33534799
chr21,33534803
chr21,33534843
chr21,33534860
chr21,33534910
chr21,33555992
chr21,33558074
chr21,33558086
chr21,33558110
chr21,33558123
chr21,33558129
chr21,33558130
chr21,33558163
chr21,33558173
chr21,33558254
chr21,33558255
SK editing
chr21,33558074
chr21,33558086
chr21,33558123
chr21,33558130
chr21,33558163
chr21,33558254
RefSeq Genes
IFNAR2
IFNAR2
IFNAR2
Human RNA Editing from the DAtabase of RNa EDiting
chr21.33542940
chr21.33558073
chr21.33558090
chr21.33558104
chr21.33558119
chr21.33558123
chr21.33558126
chr21.33558129
chr21.33558130
chr21.33558141
chr21.33558190
chr21.33558194
chr21.33558217
chr21.33558231
chr21.33558254
chr21.33558271
Repeating Elements by RepeatMasker
SINE
LINE
LTR
DNA
Simple
Low Complexity
Satellite
RNA
Other
Unknown

D

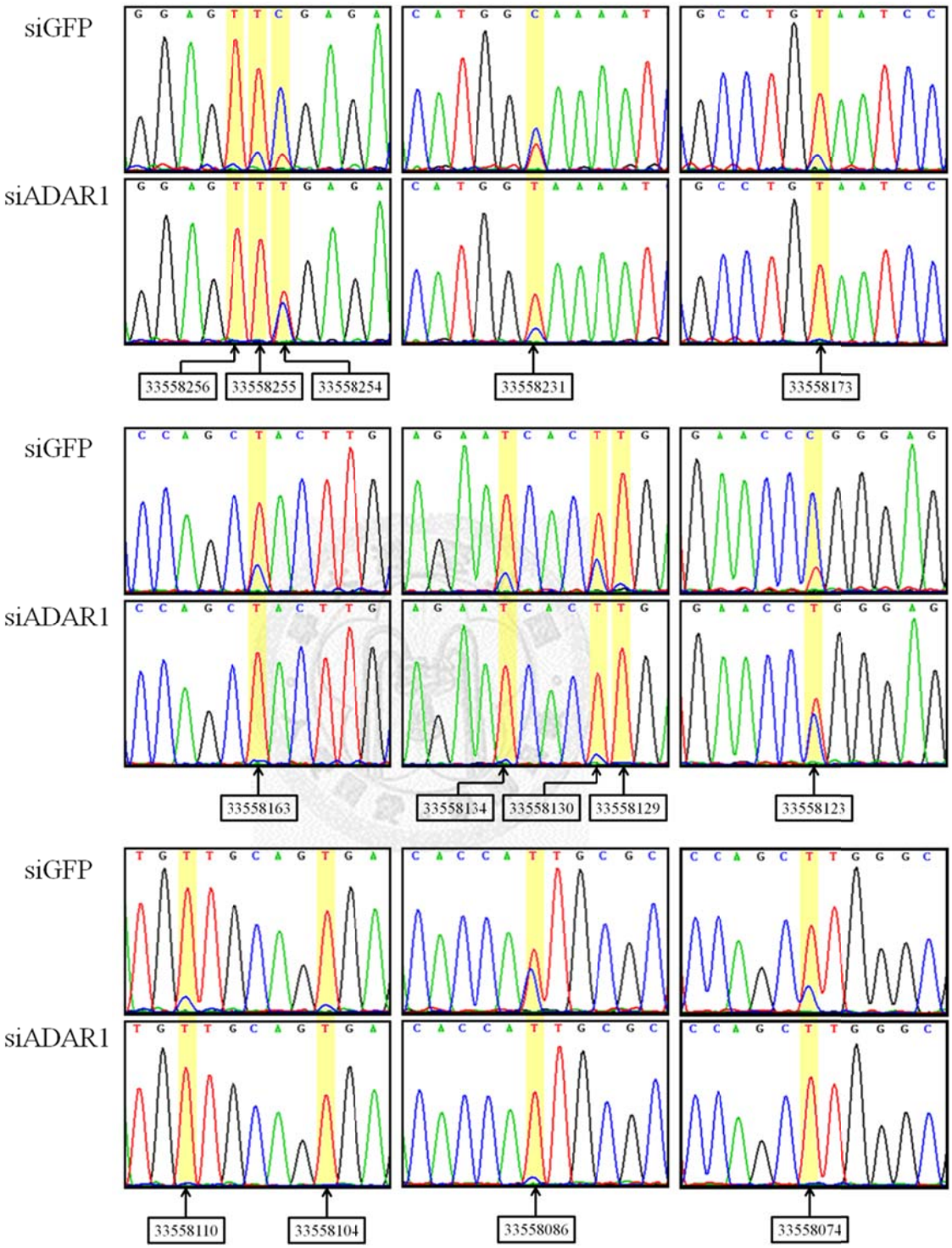
siGFP
siADAR1
33558256
33558255
33558254
33558231
33558173
siGFP
siADAR1
33558163
33558134
33558130
33558129
33558123
siGFP
siADAR1
33558110
33558104
33558086
33558074

E

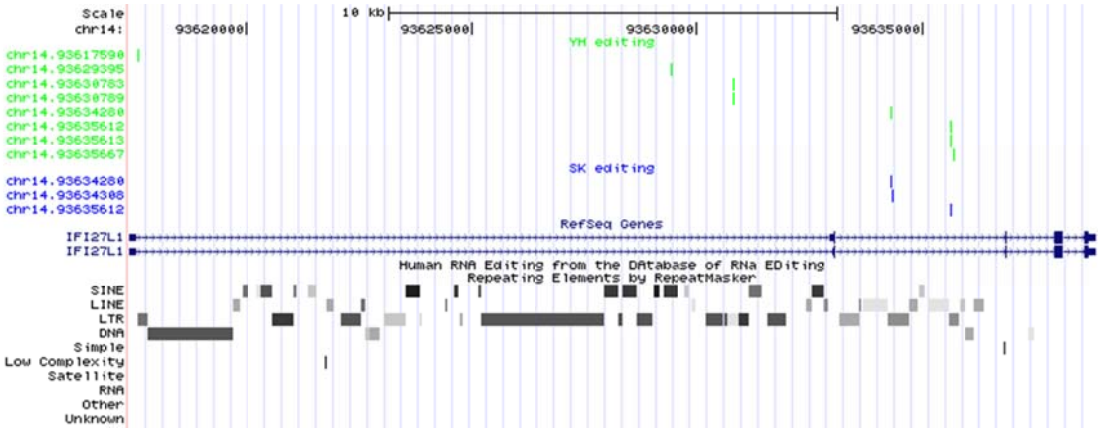
Scale
chr14:
10 kb
93620000
93625000
93630000
93635000
YH editing
chr14.93617590
chr14.93629395
chr14.93630783
chr14.93630789
chr14.93634280
chr14.93635612
chr14.93635613
chr14.93635667
SK editing
chr14.93634280
chr14.93634308
chr14.93635612
RefSeq Genes
IFI27L1
IFI27L1
Human RNA Editing from the DAtabase of RNa EDiting
Repeating Elements by RepeatMasker
SINE
LINE
LTR
DNA
Simple
Low Complexity
Satellite
RNA
Other
Unknown

F

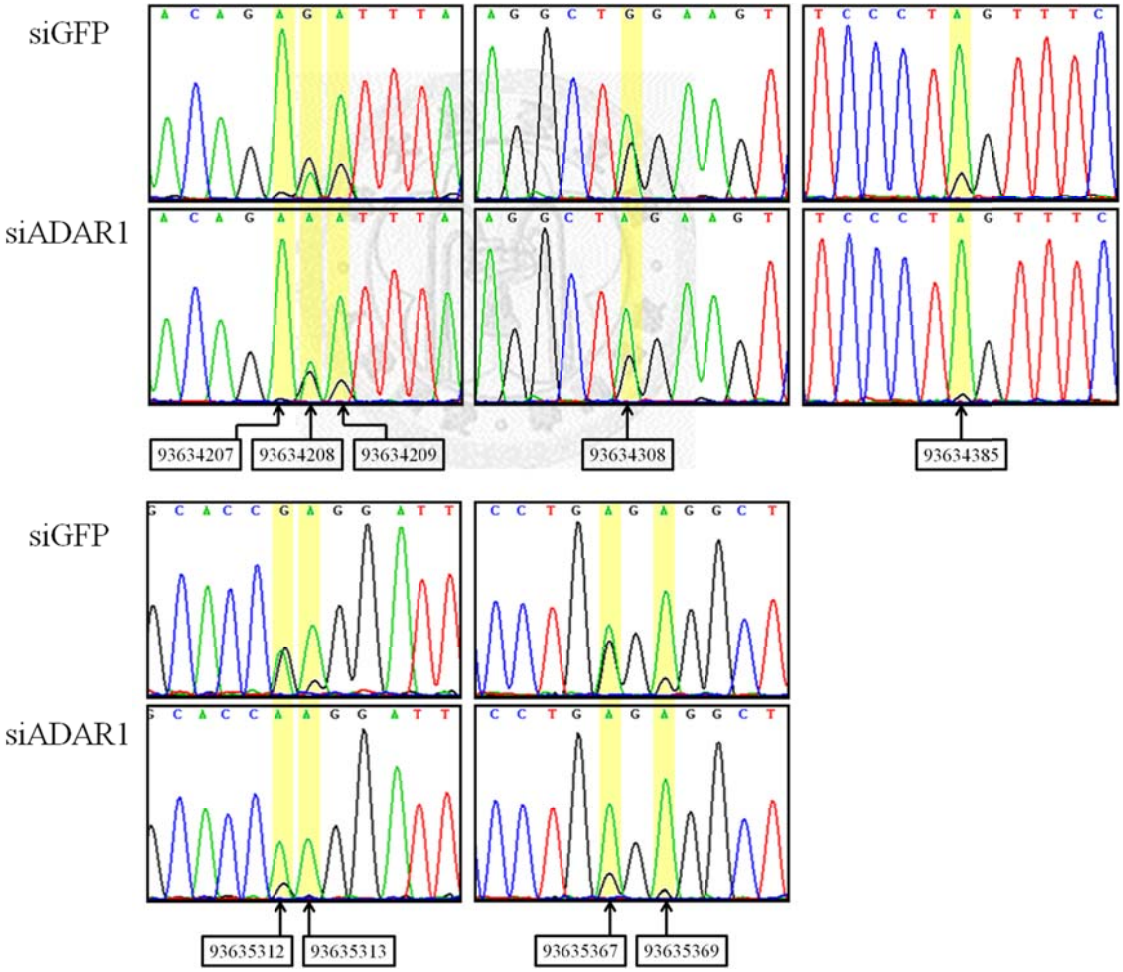
siGFP
siADAR1
93634207
93634208
93634209
93634308
93634385
siGFP
siADAR1
93635312
93635313
93635367
93635369

G

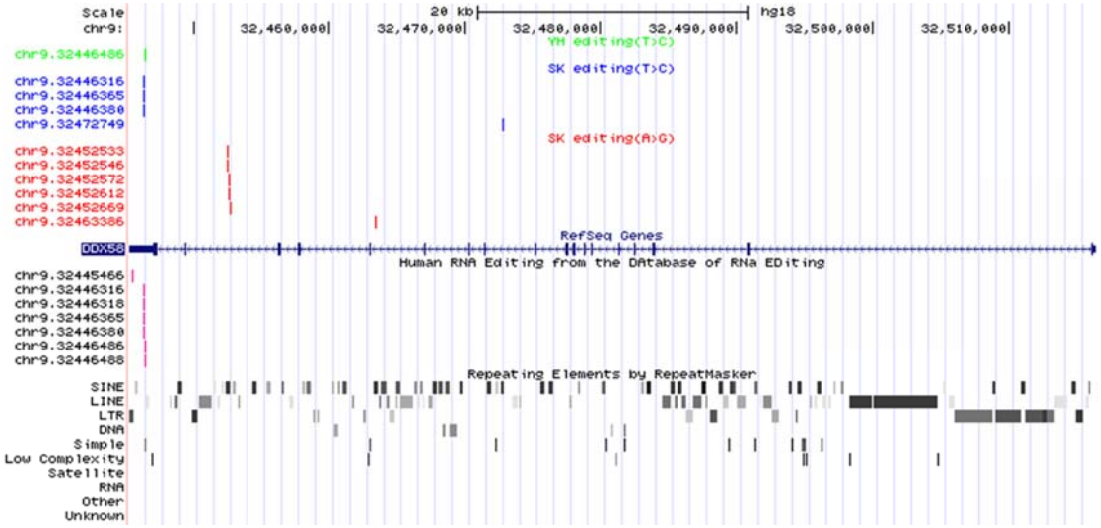
Scale
chr9:
20 kb
hg18
32,460,000
32,470,000
32,480,000
32,490,000
32,500,000
32,510,000
YH editing(T>C)
SK editing(T>C)
SK editing(A>G)
chr9.32446486
chr9.32446316
chr9.32446365
chr9.32446380
chr9.32472749
chr9.32452533
chr9.32452546
chr9.32452572
chr9.32452612
chr9.32452669
chr9.32463386
RefSeq Genes
DDX58
Human RNA Editing from the DAtabase of RNA EDiting
chr9.32445466
chr9.32446316
chr9.32446318
chr9.32446365
chr9.32446380
chr9.32446486
chr9.32446488
Repeating Elements by RepeatMasker
SINE
LINE
LTR
DNA
Simple
Low Complexity
Satellite
RNA
Other
Unknown

H

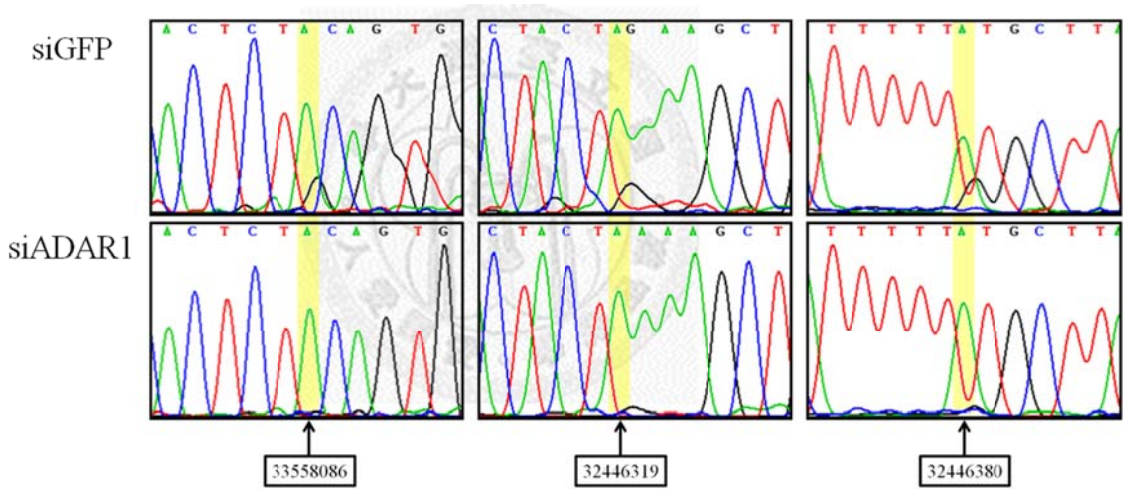
siGFP
siADAR1
33558086
32446319
32446380

I

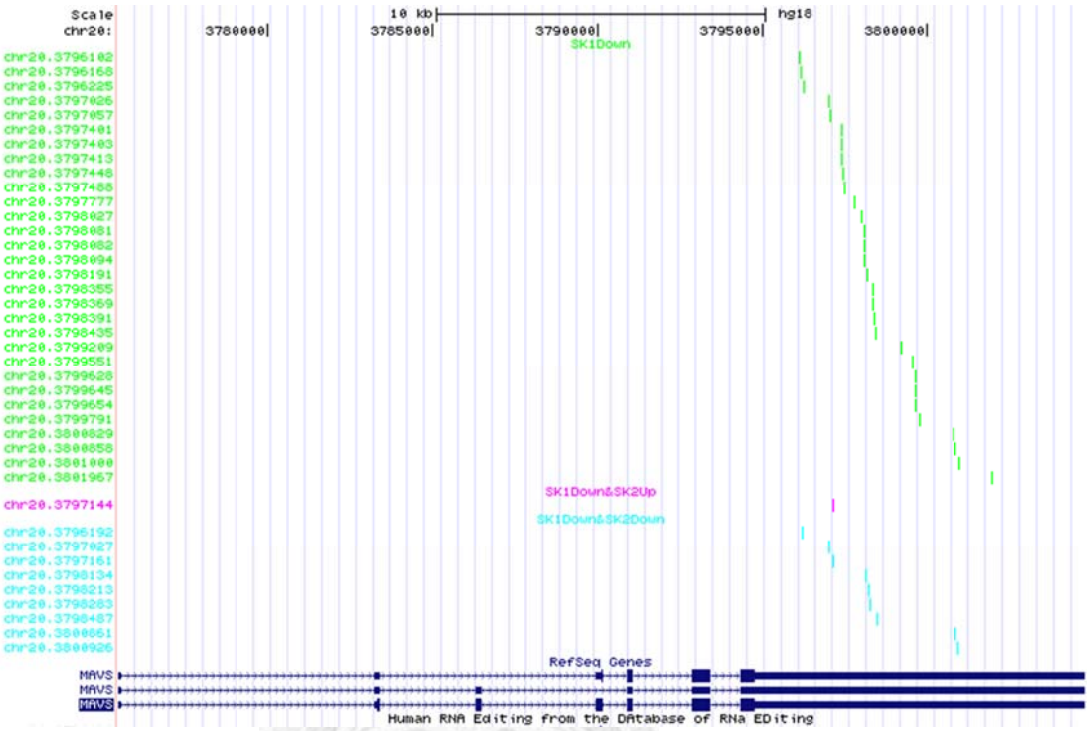
Scale
chr20:
10 kb
hg18
3780000
3785000
3790000
3795000
3800000
SK1Down
chr20.3796102
chr20.3796168
chr20.3796225
chr20.3797026
chr20.3797057
chr20.3797401
chr20.3797403
chr20.3797413
chr20.3797448
chr20.3797488
chr20.3797777
chr20.3798027
chr20.3798081
chr20.3798082
chr20.3798094
chr20.3798191
chr20.3798355
chr20.3798369
chr20.3798391
chr20.3798435
chr20.3799209
chr20.3799551
chr20.3799628
chr20.3799645
chr20.3799654
chr20.3799791
chr20.3800829
chr20.3800858
chr20.3801000
chr20.3801957
SK1Down&SK2Up
chr20.3797144
SK1Down&SK2Down
chr20.3796192
chr20.3797027
chr20.3797161
chr20.3798134
chr20.3798213
chr20.3798283
chr20.3798487
chr20.3800661
chr20.3800926
RefSeq Genes
MAVS
MAVS
MAVS
Human RNA Editing from the DAtabase of RNa EDiting

J

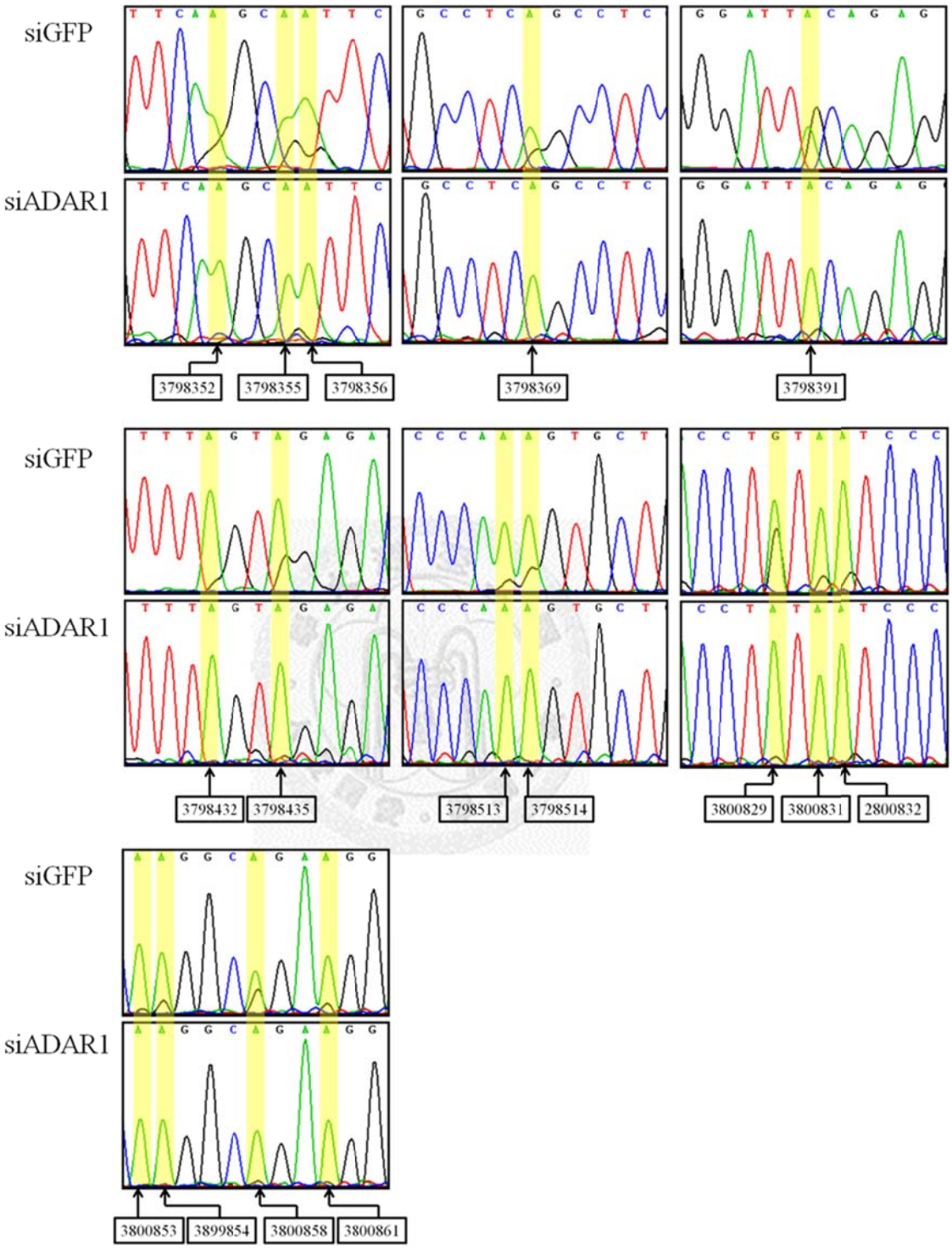
siGFP
siADAR1
3798352
3798355
3798356
3798369
3798391
siGFP
siADAR1
3798432
3798435
3798513
3798514
3800829
3800831
2800832
siGFP
siADAR1
3800853
3899854
3800858
3800861

K

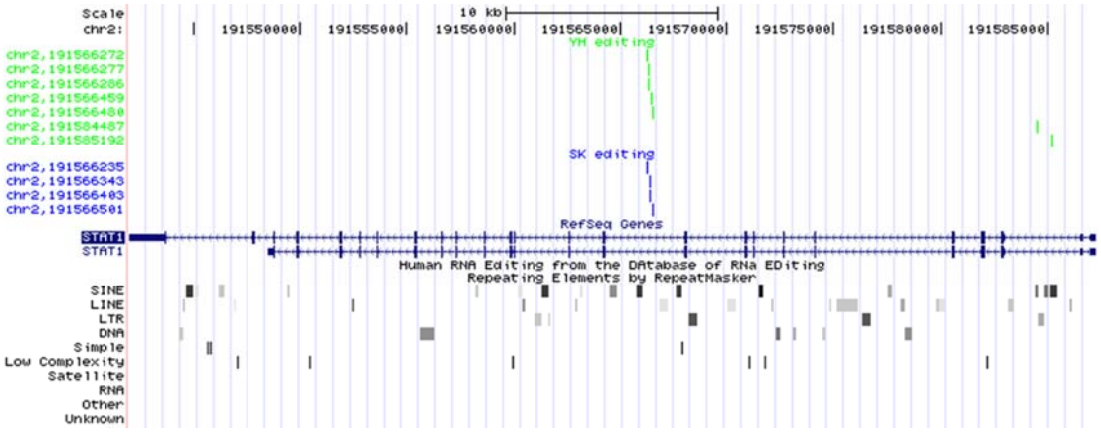
Scale
chr2:
10 kb
191550000
191555000
191560000
191565000
191570000
191575000
191580000
191585000
YH editing
chr2,191566272
chr2,191566277
chr2,191566286
chr2,191566459
chr2,191566480
chr2,191584487
chr2,191585192
SK editing
chr2,191566235
chr2,191566343
chr2,191566403
chr2,191566501
RefSeq Genes
STAT1
STAT1
Human RNA Editing from the DAtabase of RNa EDiting
Repeating Elements by RepeatMasker
SINE
LINE
LTR
DNA
Simple
Low Complexity
Satellite
RNA
Other
Unknown

L

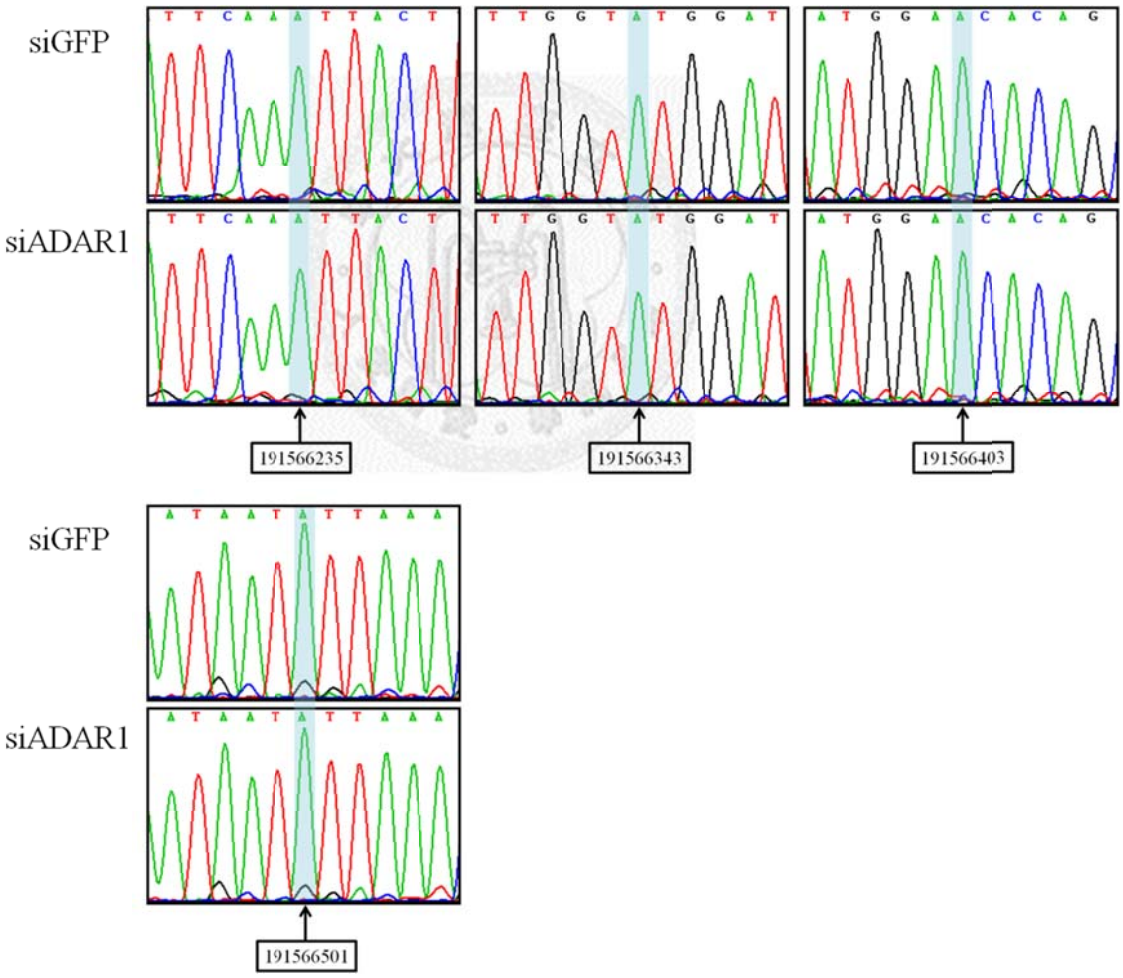
siGFP
siADAR1
191566235
191566343
191566403
siGFP
siADAR1
191566501

M

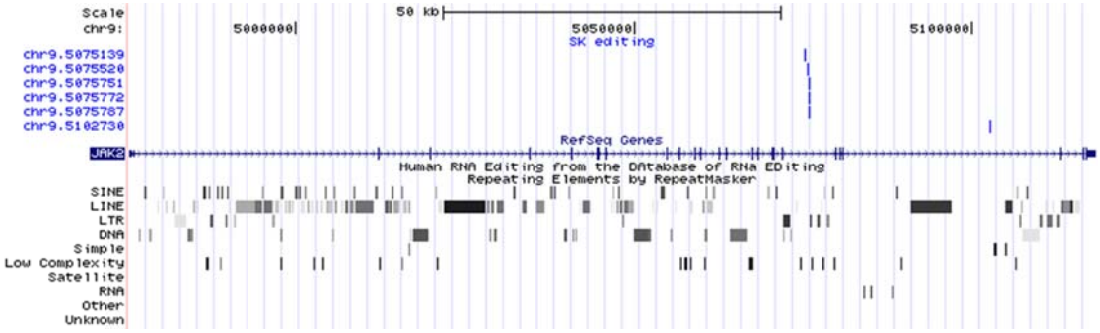
Scale
chr9:
50 kb
5000000
5050000
5100000
SK editing
chr9.5075139
chr9.5075520
chr9.5075751
chr9.5075772
chr9.5075787
chr9.5102730
RefSeq Genes
JAK2
Human RNA Editing from the DNtabase of RNA EDiting
Repeating Elements by RepeatMasker
SINE
LINE
LTR
DNA
Simple
Low Complexity
Satellite
RNA
Other
Unknown

N

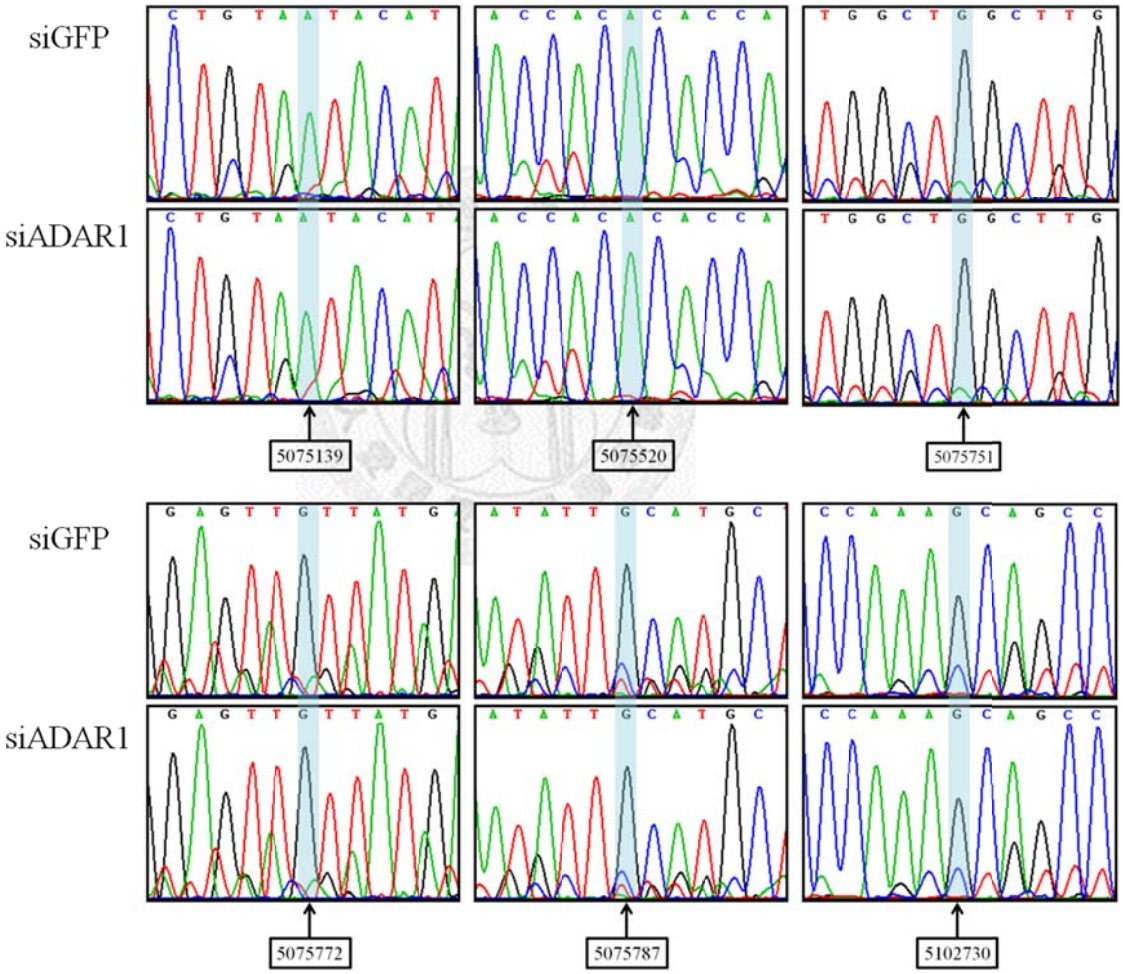
siGFP
siADAR1
5075139
5075520
5075751
siGFP
siADAR1
5075772
5075787
5102730

Figure 1. Ratio of RNA adenine to inosine editing of IFNAR1, IFNAR2, IFI27L1, DDX58 and MAVS were decreased after ADAR1 knockdown.

The predicted editing sites of our NGS data were labeled through UCSC database. The transcript of plus-strand genes were represented by blue line with right arrow, and of minus-strand genes were represented by blue line with left arrow; in addition, 3' UTR, 5' UTR and exons were symbolized as rectangles. The editing sites based on our NGS data were labeled on upper panel. The bottom panel indicated the editing sites published by other literatures, and repeated sequences with gray rectangles (A, C, E, G, I, K and M). The predicted editing sites were confirmed by Sanger sequencing. The nucleotides highlighted by yellow column were the sites where the A to I events were decreased after ADAR1 knockdown. On the other hand, the nucleotides highlighted by blue column were the predicted sites with no editing events having being observed (B, D, F, H and J).

A

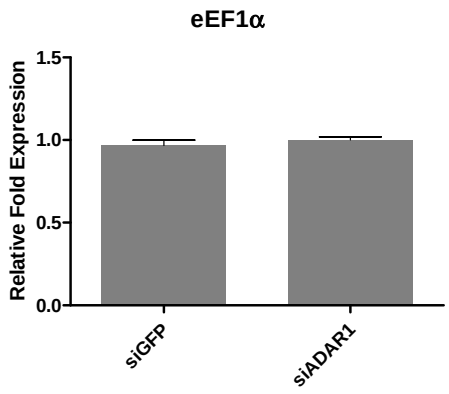
eEF1α
Relative Fold Expression
1.5
1.0
0.5
0.0
siGFP
siADAR1

B

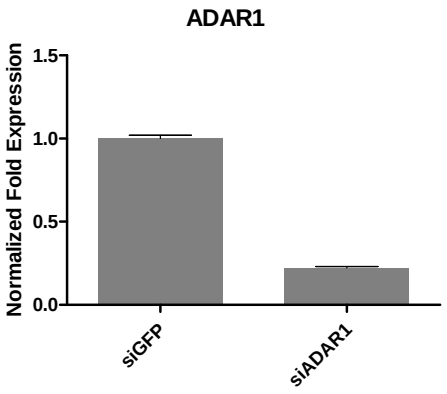
ADAR1
Normalized Fold Expression
1.5
1.0
0.5
0.0
siGFP
siADAR1

C

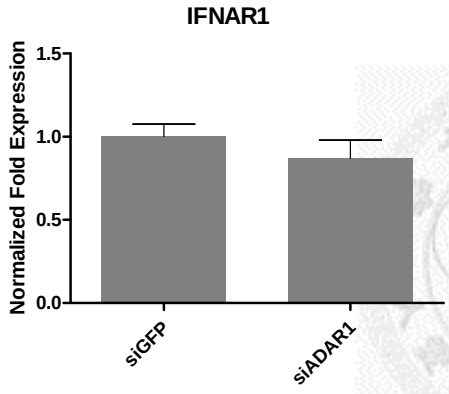
IFNAR1
Normalized Fold Expression
1.5
1.0
0.5
0.0
siGFP
siADAR1

D

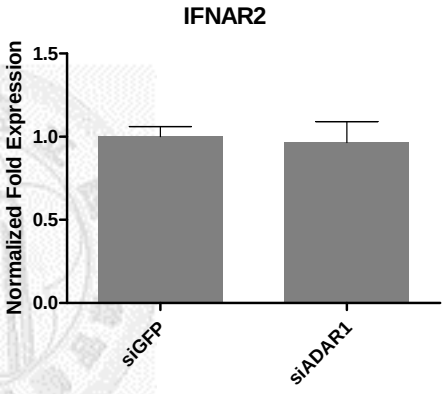
IFNAR2
Normalized Fold Expression
1.5
1.0
0.5
0.0
siGFP
siADAR1

B

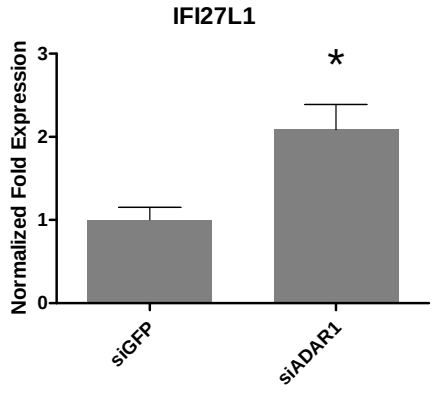
IFI27L1
Normalized Fold Expression
3
2
1
0
*
siGFP
siADAR1

F

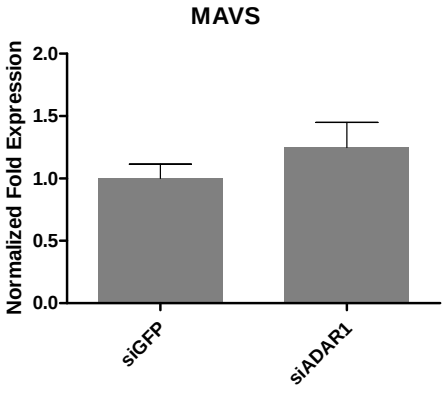
MAVS
Normalized Fold Expression
2.0
1.5
1.0
0.5
0.0
siGFP
siADAR1

Figure 2. RNA expression level of target genes were not altered after ADAR1 knockdown, except for IFI27L1.

SK-N-SH cells were transfected by siRNA specific to GFP or ADAR1, and RNA samples were harvested 48 hours after transfection. The sequence of primers we used to detect mRNA expression level through qPCR was described in table 1. After ADAR1 knockdown, the internal control, eEF1α expressed at constant level (A), and the knockdown efficiency of ADAR1 was 80% (B). The expression level of IFNAR1, IFNAR2 and MAVS remained equal under these two conditions (C, D and F); however, IFI27L1 was statistically significantly increased (E). $P < 0.05$.

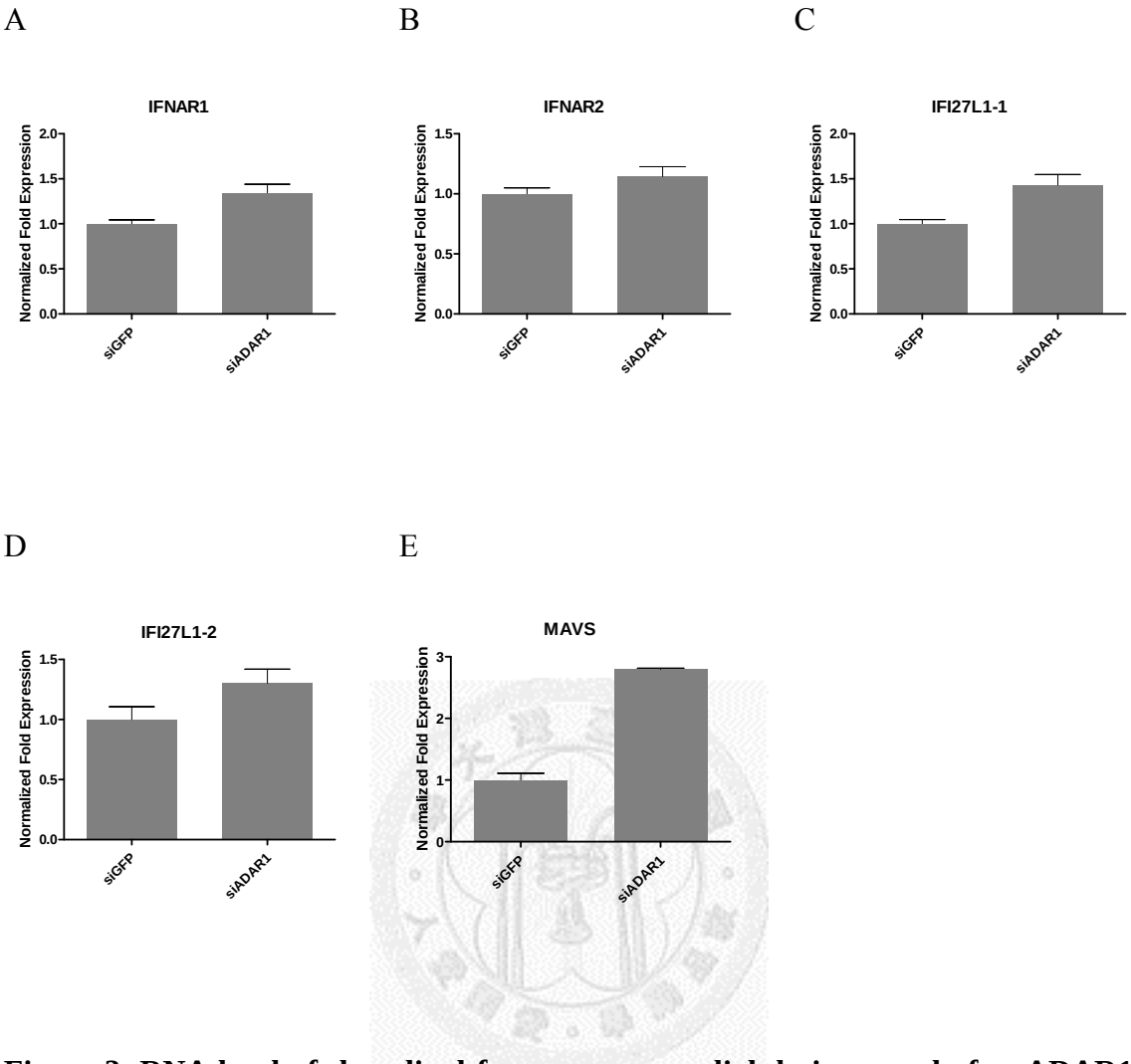

Figure 3. RNA level of the edited fragments were slightly increased after ADAR1 knockdown.

The experimental materials and methods had been mentioned in figure 2. Differed with mRNA, the expression levels of edited fragments of IFNAR1, IFNAR2 IFI27L1 and MAVS were increase after ADAR1 knockdown.

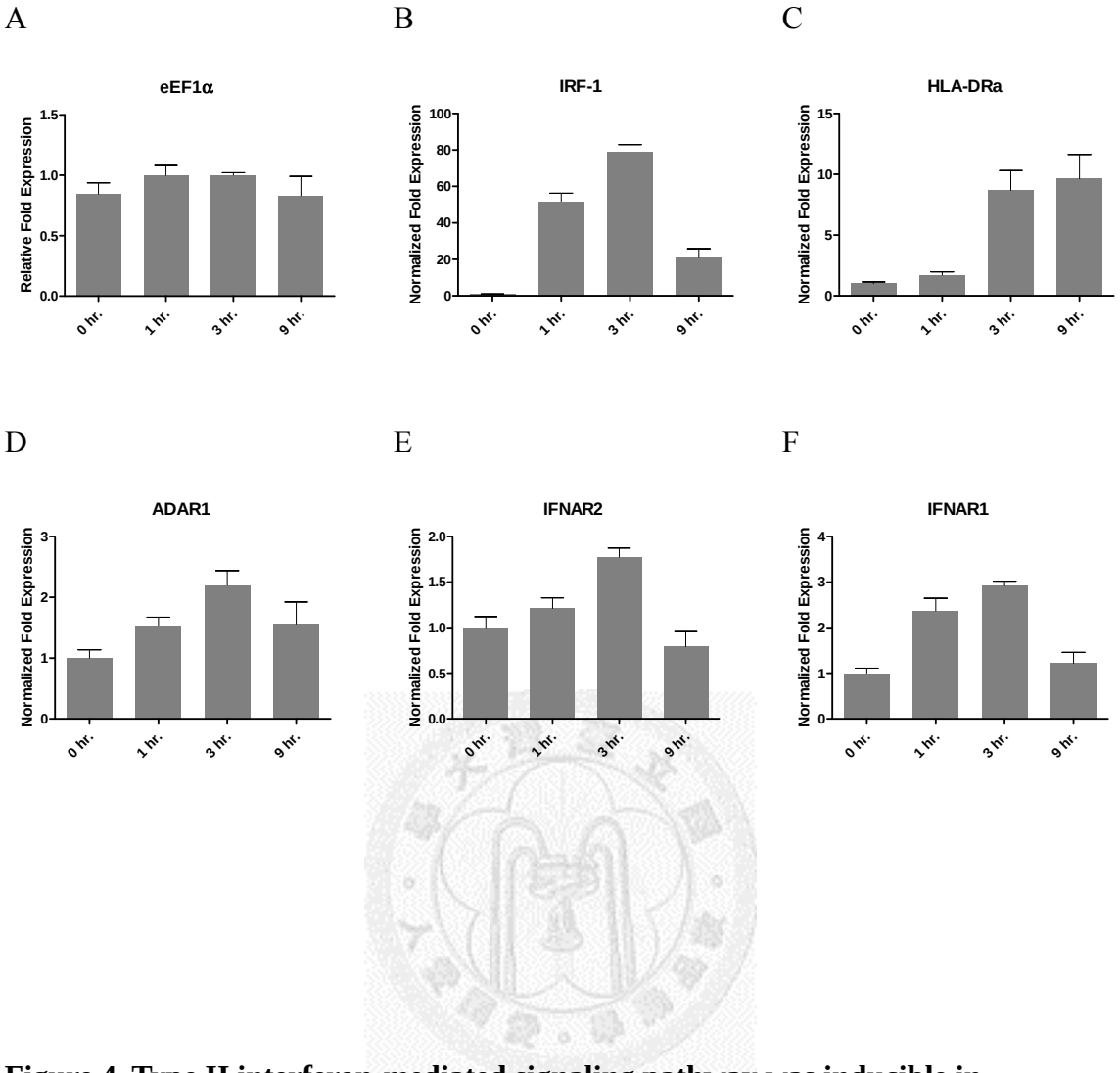

Figure 4. Type II interferon-mediated signaling pathway was inducible in SK-N-SH cell.

When SK-N SH cells grew in 90% confluence, RNA samples were harvested after the treatment of interferon-gamma (20 ng/mL) for 0, 1, 3 or 9 hours, and the expression level of target genes were measured by qPCR. The internal control was eEF1α (A), and the positive controls we used were IRF-1 (B) and HLA-DRα (C). Consistent with previous reports, the mRNA expression levels of IFNAR1 (D), IFNAR2 (E) , ADAR1 (F) and PRKRA (G) were increased after IFN-gamma treatment.

A

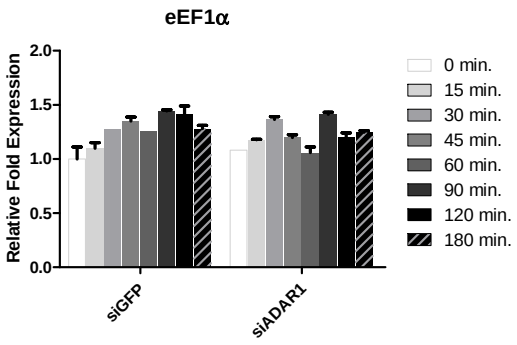
eEF1α
Relative Fold Expression
2.0
1.5
1.0
0.5
0.0
siGFP
siADAR1
0 min.
15 min.
30 min.
45 min.
60 min.
90 min.
120 min.
180 min.

B

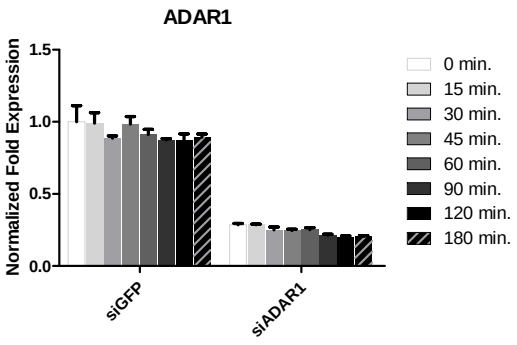
ADAR1
Normalized Fold Expression
1.5
1.0
0.5
0.0
siGFP
siADAR1
0 min.
15 min.
30 min.
45 min.
60 min.
90 min.
120 min.
180 min.

C

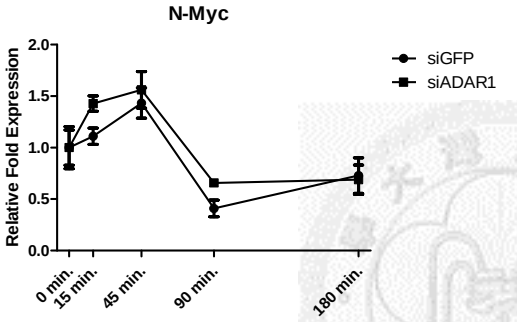
N-Myc
Relative Fold Expression
2.0
1.5
1.0
0.5
0.0
0 min.
15 min.
45 min.
90 min.
180 min.
siGFP
siADAR1

D

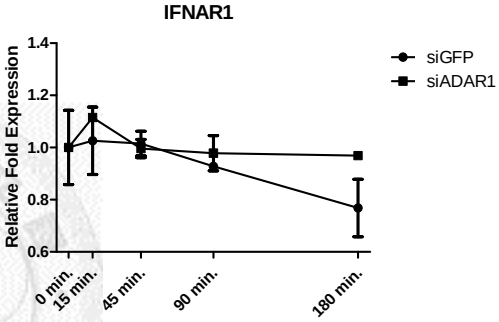
IFNAR1
Relative Fold Expression
1.4
1.2
1.0
0.8
0.6
0 min.
15 min.
45 min.
90 min.
180 min.
siGFP
siADAR1

E

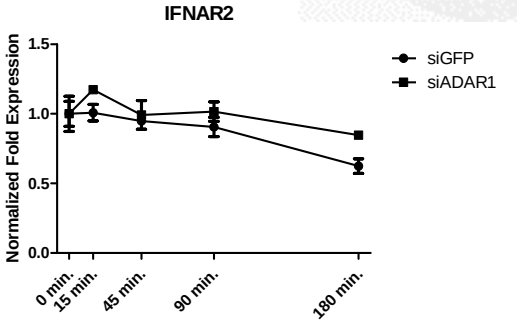
IFNAR2
Normalized Fold Expression
1.5
1.0
0.5
0.0
0 min.
15 min.
45 min.
90 min.
180 min.
siGFP
siADAR1

F

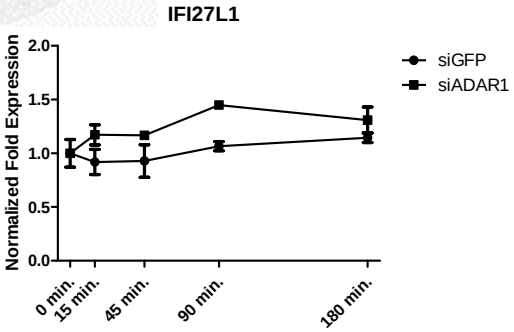
IFI27L1
Normalized Fold Expression
2.0
1.5
1.0
0.5
0.0
0 min.
15 min.
45 min.
90 min.
180 min.
siGFP
siADAR1

G

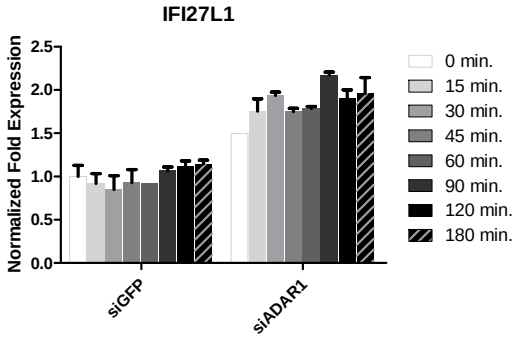

Figure 5. RNA stability of genes involved in JAK/STAT pathway remained equal after ADAR1 knockdown.

SK-N-SH cells were transfected by siRNA specific to GFP or ADAR1 for 48 hours, then cells were treated with IFN-gamma (20 ng/mL) for 3 hours. Finally, the RNA samples were harvested after actinomycin D (10 μg/mL) treatment for 0, 15, 45, 90 and 180 minutes. The internal control, eEF1α, expressed at constant level under this condition (A). The knockdown efficiency of ADAR1 was 80% (B). The positive control we used was N-myc, which was dramatically decreased 45 minutes after treatment with actinomycin D (C). However, RNA stability of IFNAR1 (D), IFNAR2 (E) and IFI27L1 (F) remained stable even 180 minutes after actinomycin D treatment. In addition, mRNA expression level of IFI27L1 was increased after ADAR1 knockdown (G), consistent with previous data (fig. 2E).

A

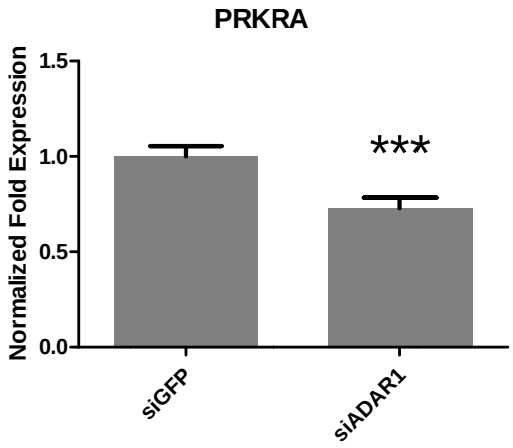

B

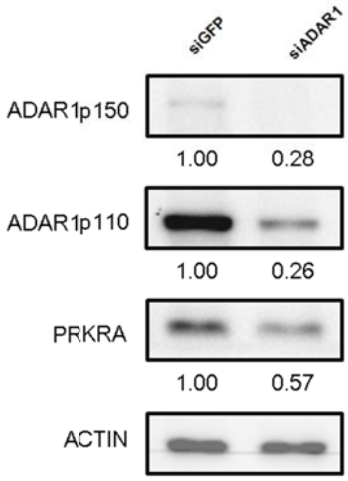

Figure 6. Both protein and mRNA expression of PRKRA was decreased after ADAR1 knockdown.

Cell lysates and cell homogenates of SK-N-SH cells were harvested 48 hours after siRNA transfection. After ADAR1 knockdown, mRNA expression level of PRKRA was decreased by 30 percents (A). In addition, protein level of PRKRA was decreased by 40 percents (B).

A

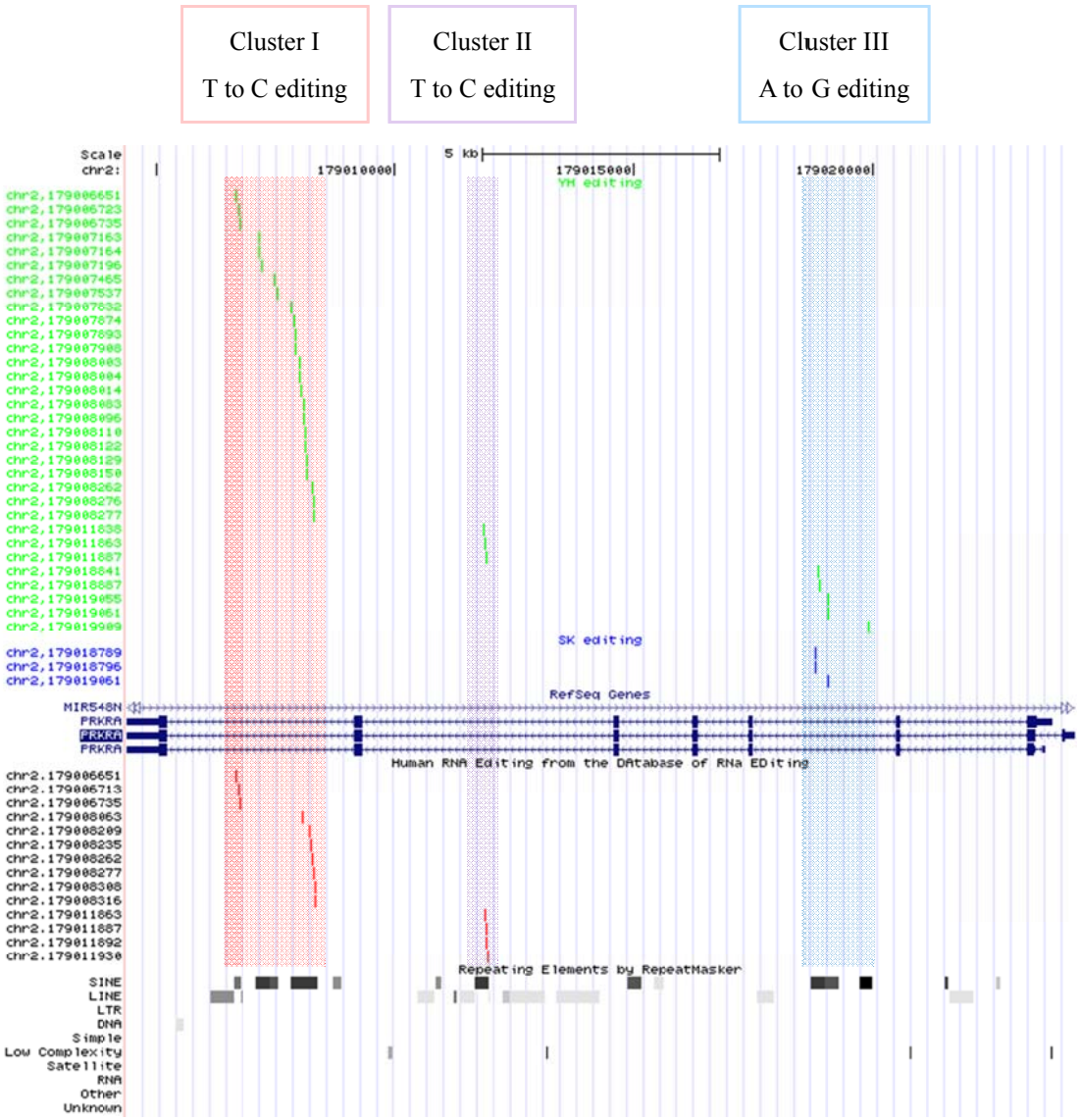
Cluster I
T to C editing
Cluster II
T to C editing
Cluster III
A to G editing
Scale
chr2:
5 kb
179010000
179015000
179020000
YH editing
SK editing
RefSeq Genes
MIR548N
PRKRA
Human RNA Editing from the DAtabase of RNa EDiting
Repeating Elements by RepeatMasker
SINE
LINE
LTR
DNA
Simple
Low Complexity
Satellite
RNA
Other
Unknown

B

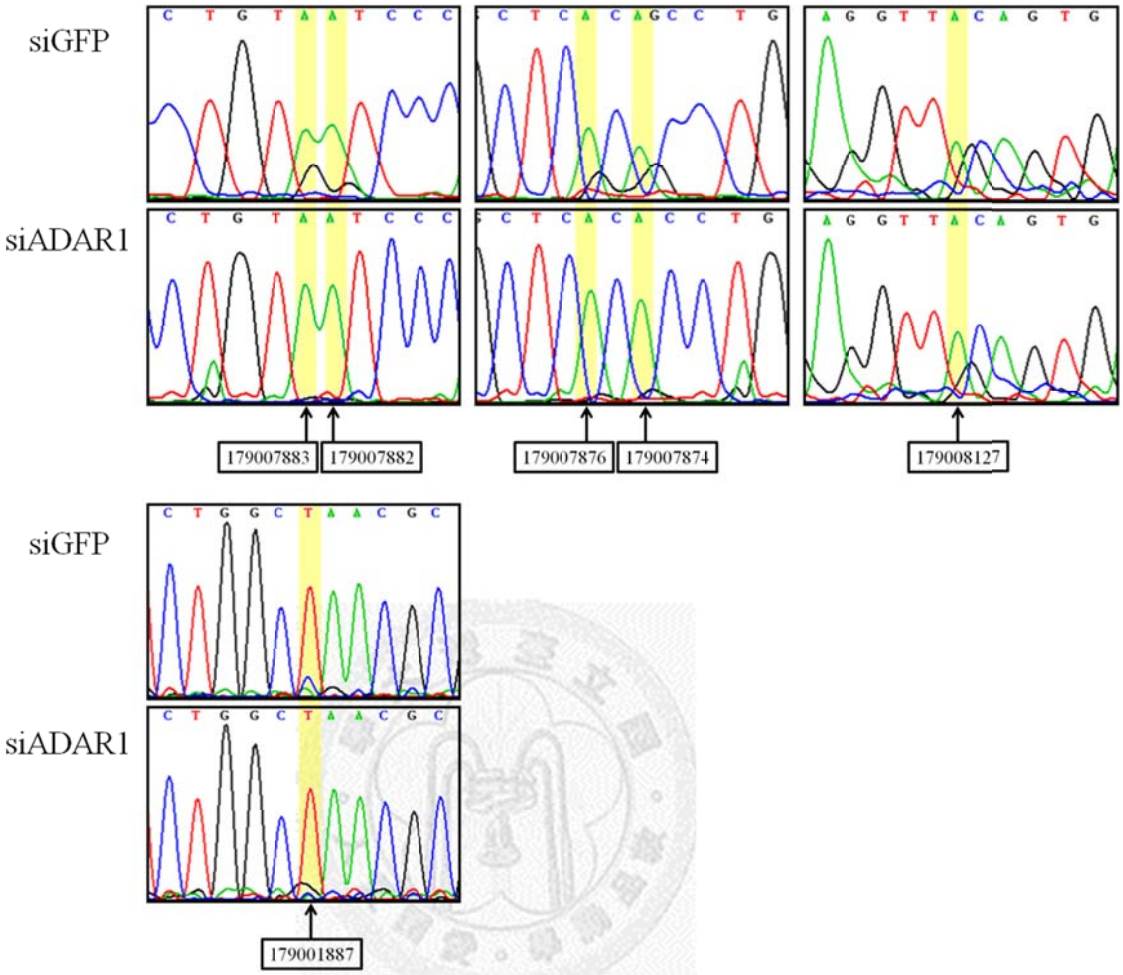
siGFP
siADAR1
179007883
179007882
179007876
179007874
179008127
siGFP
siADAR1
179001887

Figure 7. T to C editing events in intron neighboring 3' end of PRKRA transcript were confirmed by Sanger sequencing.

The predicted editing sites were labeled in UCSC database, and the details were mentioned in figure 1. The editing sites were classified into 3 clusters, and editing sites belonged to cluster I and II showed T to C editing events. In contrary, editing sites belonged to cluster III showed A to G editing events (A). The predicted editing sites were confirmed by Sanger sequencing. The nucleotides highlight by yellow column show where the A to I events were decreased after ADAR1 knockdown (B).

A

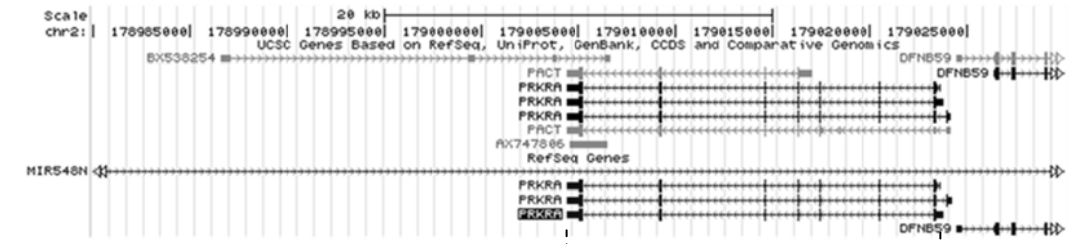

B

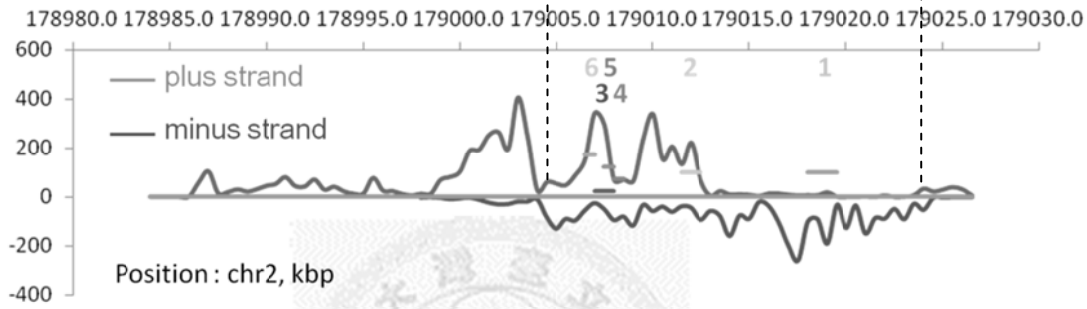

C

Cluster I II III

Figure 8. Information from UCSC and GBrowser database indicated the existence of the antisense transcript.

The information of PRKRA were obtained from UCSC database (A and C) and GBrowser database (B). According to these information, the position of PRKRA in chromosome was correlated with the reads number we counted in GBrowser database (A and B, dotted line). Moreover, the GBrowser database indicated there was an antisense transcript which overlapped with PRKRA transcript and was located in plus strand might be expressed (B). Based on our NGS data, editing sites contained in PRKRA transcript were classified into three clusters (C), and 6 pairs of primers were designed for following experiments (B). It's worth noting that editing sites in cluster I and II were located on the antisense transcript, but editing sites in cluster III is located on PRKRA transcript.

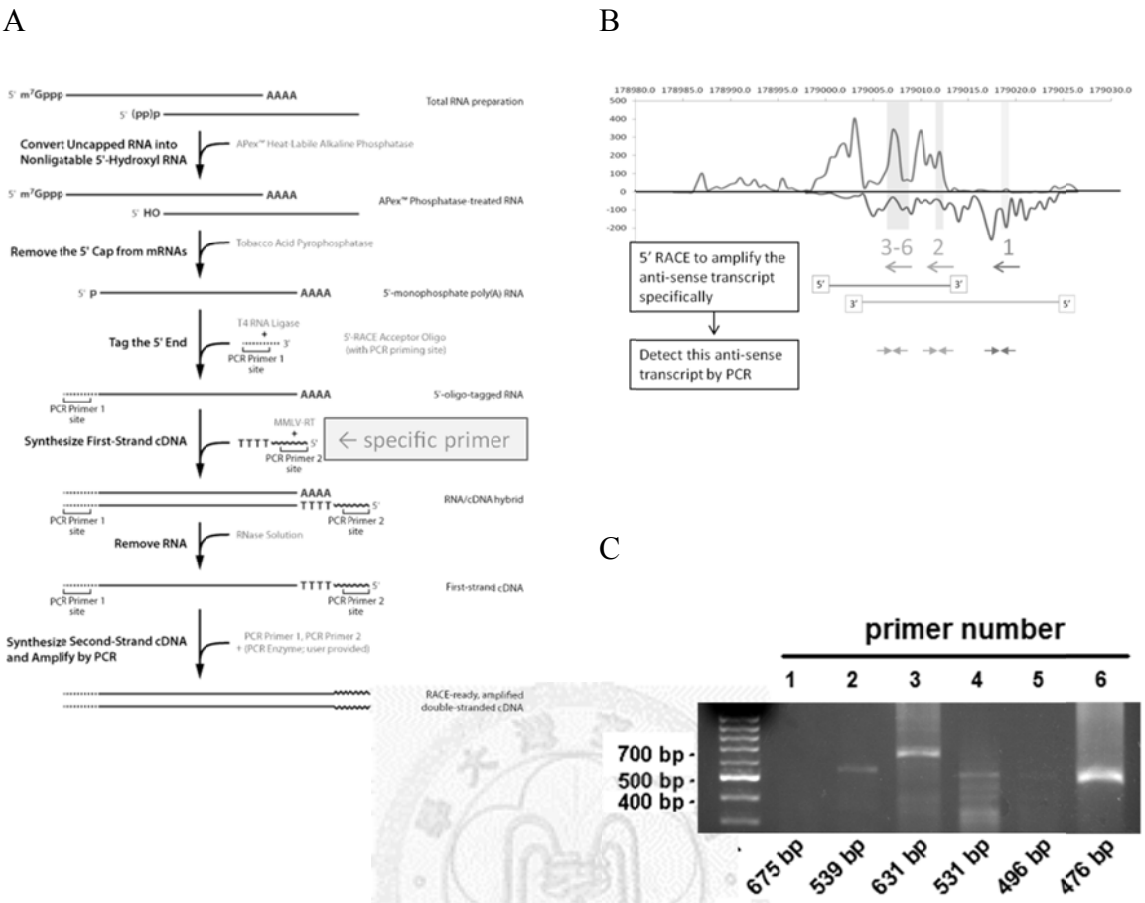

Figure 9. The existence of antisense transcript was confirmed by 3' RACE.

The flowchart of the RACE protocol we followed was mentioned in ExactSTART™ Eukaryotic mRNA 5'- & 3'-RACE Kit, and more details had been described in chapter 2.9 (A) The primers we used for this RACE experiment were designed based on the information we obtained from figure 8 (B), and the results were confirmed by end-point PCR. Signals of PCR products of primer 2 to 6, which were located in overlapped region between PRKRA and the antisense transcript, but for primer 1 were detectable (C).

Fig. 10

A

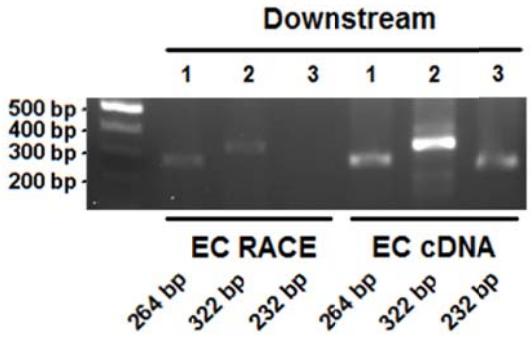

B

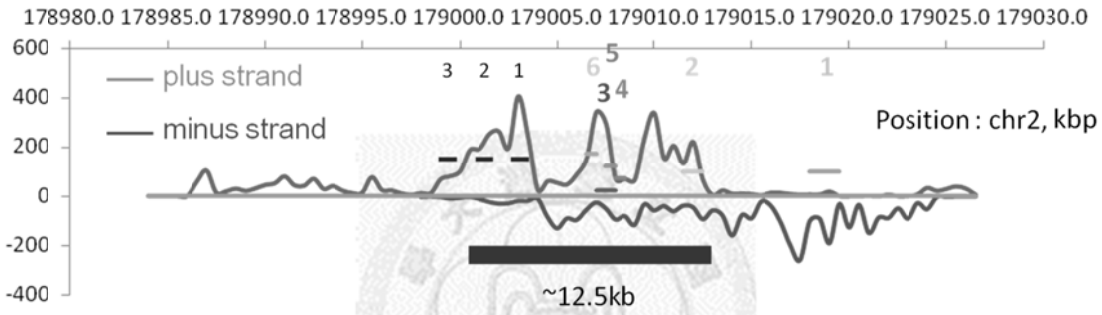

Figure 10. The signal of the antisense transcript was detected downstream of the PRKRA transcript.

Three primers were designed downstream of the PRKRA transcript, and the results are confirmed by end-point PCR. Signals of PCR products of these three primers were detectable when whole genome cDNA of EC was used as DNA template, but the signal of primer 3 was eliminated when EC RACE was used as template (A). Combing these data with the information of Gbrowser database, the predicted position of the antisense transcript was about 12.5 kb based on these results.

A

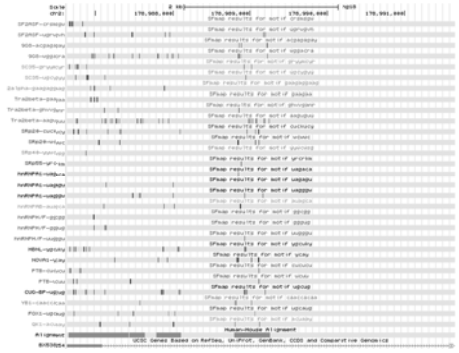

B

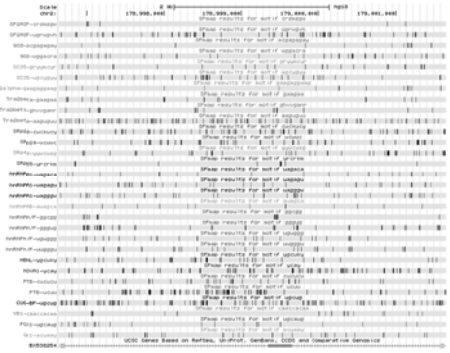

C

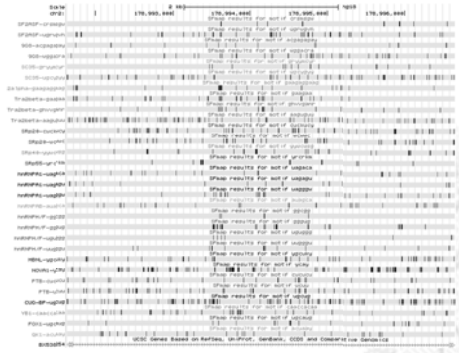

D

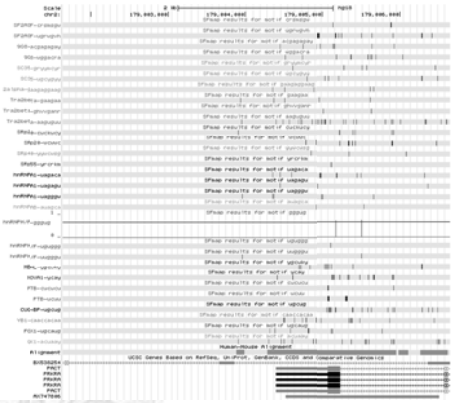

Figure 11. The predicted splicing binding sites were abundant in the antisense transcript.

The splicing factor binding sites were predicted through SFmap database. Each figures contain 5,000 nucleotides according to the sequence of the antisense transcript, and . 5' region (A) and 3' (D) region of the antisense transcript contained much less splicing factor binding sites compared to the middle region (B and C).

A

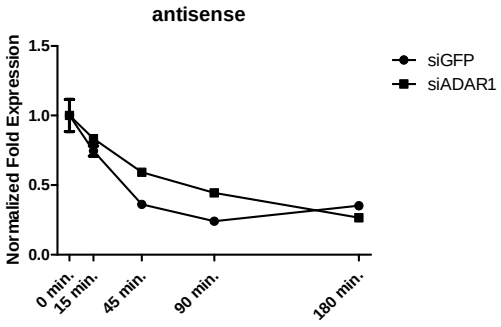

B

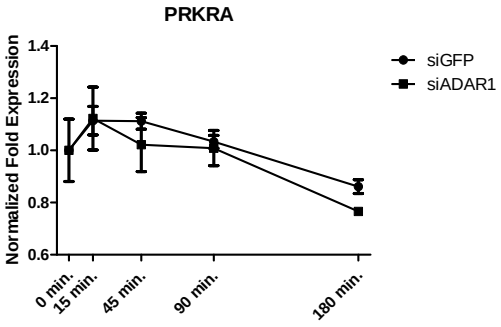

Figure 12. The half-life time of the antisense transcript was prolonged after ADAR1 knockdown.

The RNA stability was measured at 0, 15, 45, 90 and 180 minutes after actinomycin D treatment, as we mentioned in figure 5. The RNA half-life time of the antisense transcript was increased from 30 minutes to 90 minutes after ADAR1 knockdown (A), but no significant change of RNA stability of PRKRA had been observed after ADAR1 knockdown (B).

A

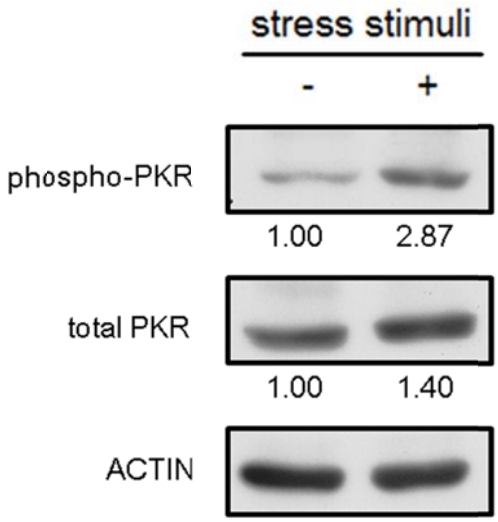

Figure 13. Ratio of pPKR to PKR was increased under the stress stimulation.

SK-N-SH cells were treated with 50 ng/mL actinomycin D in serum-free medium for 1 hour in 90% confluence, then the cell lysates were harvested by WCE buffer. The protein expression of total PKR was slightly increased, and phosphorylated PKR were up-regulated threefold after the stress stimuli.

A

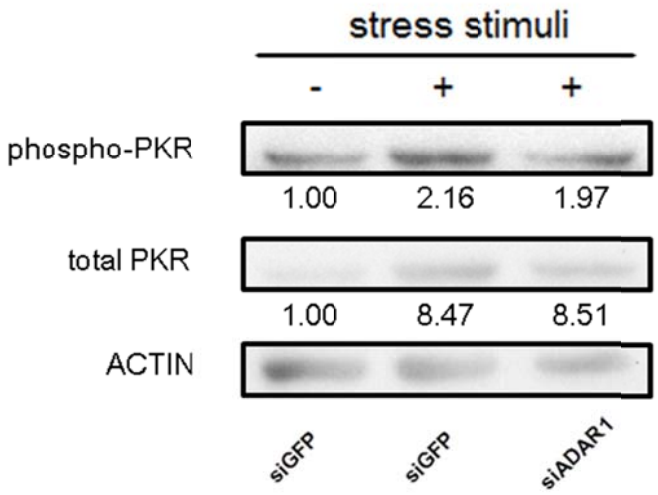

Figure 14. Ratio of pPKR to PKR was increased under stress stimulation after ADAR1 knockdown, but not as much as control group.

SK-N-SH cells were treated with or without stress stimuli for 1 hour after siRNA transfection, then cell lysates were harvested by WCE buffer. The protein expression level of total PKR and phosphorylated PKR were increased after stress stimuli, but no obvious differences were observed between control and ADAR1 knockdown groups.

A

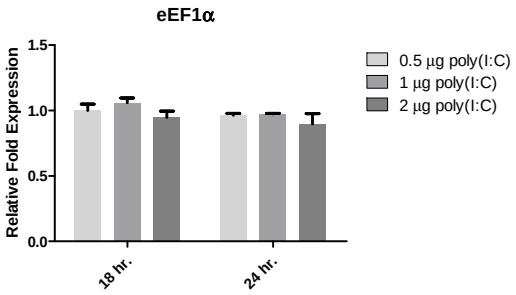
eEF1α
Relative Fold Expression
1.5
1.0
0.5
0.0
18 hr.
24 hr.
0.5 μg poly(I:C)
1 μg poly(I:C)
2 μg poly(I:C)

B

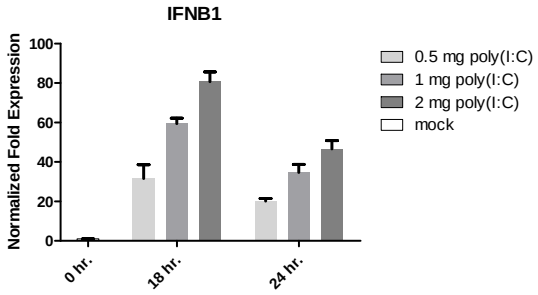
IFNB1
Normalized Fold Expression
100
80
60
40
20
0
0 hr.
18 hr.
24 hr.
0.5 mg poly(I:C)
1 mg poly(I:C)
2 mg poly(I:C)
mock

C

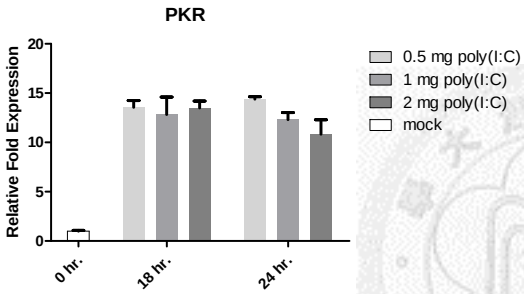
PKR
Relative Fold Expression
20
15
10
5
0
0 hr.
18 hr.
24 hr.
0.5 mg poly(I:C)
1 mg poly(I:C)
2 mg poly(I:C)
mock

D

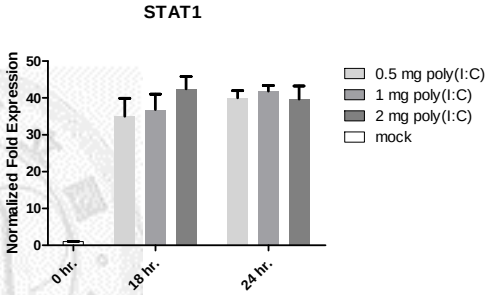
STAT1
Normalized Fold Expression
50
40
30
20
10
0
0 hr.
18 hr.
24 hr.
0.5 mg poly(I:C)
1 mg poly(I:C)
2 mg poly(I:C)
mock

Figure 15. RLR signaling pathway was inducible after poly(I:C) treatment.

SK-N-SH cells were transfected with or without poly(I:C) (0.5, 1 or 2 μg/mL) for 18 or 24 hours, and the detailss were described in chapter 2.1. The cell homogenates were harvested by TRIzol® reagent. The internal control was eEF1α, which expressed in constant during poly(I:C) treatment (A), and positive controls we used were IFNB1 (B), PKR (C) and STAT1 (D), which were dramatically raised after poly(I:C) treatment. The mRNA expression level was detected by qPCR. Although IFNB1, PKR and STAT1 were up-regulated, only IFNB1 was increased in a dose dependant manner, and the highest expression was detected when cells were treated with 2 μg/mL poly(I:C) for 18 hours.

A

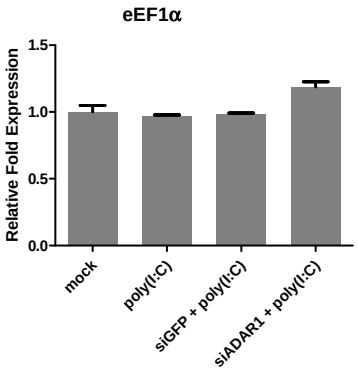
eEF1α
Relative Fold Expression
1.5
1.0
0.5
0.0
mock
poly(I:C)
siGFP + poly(I:C)
siADAR1 + poly(I:C)

B

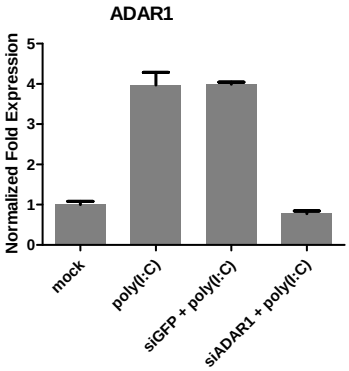
ADAR1
Normalized Fold Expression
5
4
3
2
1
0
mock
poly(I:C)
siGFP + poly(I:C)
siADAR1 + poly(I:C)

C

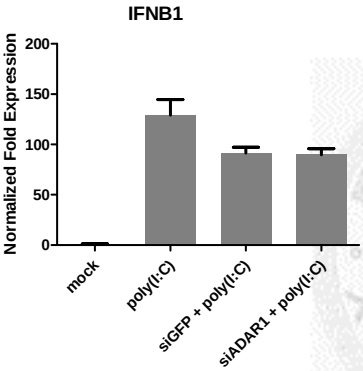
IFNB1
Normalized Fold Expression
200
150
100
50
0
mock
poly(I:C)
siGFP + poly(I:C)
siADAR1 + poly(I:C)

D

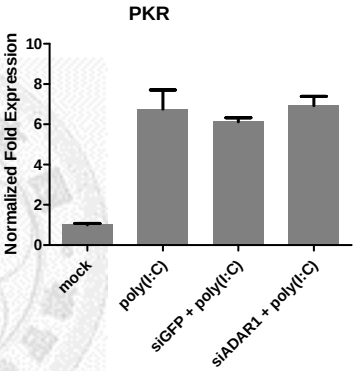
PKR
Normalized Fold Expression
10
8
6
4
2
0
mock
poly(I:C)
siGFP + poly(I:C)
siADAR1 + poly(I:C)

E

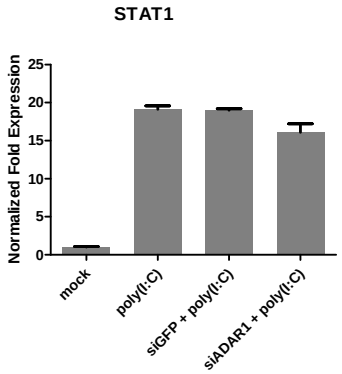
STAT1
Normalized Fold Expression
25
20
15
10
5
0
mock
poly(I:C)
siGFP + poly(I:C)
siADAR1 + poly(I:C)

Figure 16. mRNA expression of IFNB1 induced by poly(I:C) transfection was not altered after ADAR1 knockdown.

48 hours after siRNA transfection, SK-N-SH cells were treated with poly(I:C) (2 μg/mL) for 24 hours. The internal control was eEF1α (A), and the ADAR1 knockdown efficiency had been confirmed (B). mRNA expression level of IFNB1 (C), PKR (D) and STAT1 (E) were measured by qPCR under control or ADAR1 knockdown condition. Even siRNA transfection reduced the efficiency of poly(I:C) transfection, mRNA expressions of STAT1, PKR and IFNB1 were up-regulated, and no significant differences had been observed between control and ADAR1 knockdown groups.

A. B.

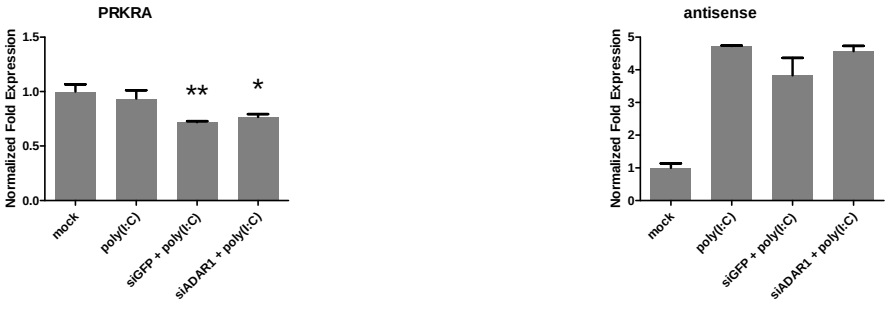

Figure 17. mRNA expression of the antisense transcript was increased after poly(I:C) transfection.

SK-N-SH cells were treated with poly(I:C) for 24 hours after siRNA transfection, as described in figure 16. After poly(I:C) treatment, mRNA expression of PRKRA was statistically significantly decreased (A), and the expression of antisense transcript was up-regulated about fivefold (B).

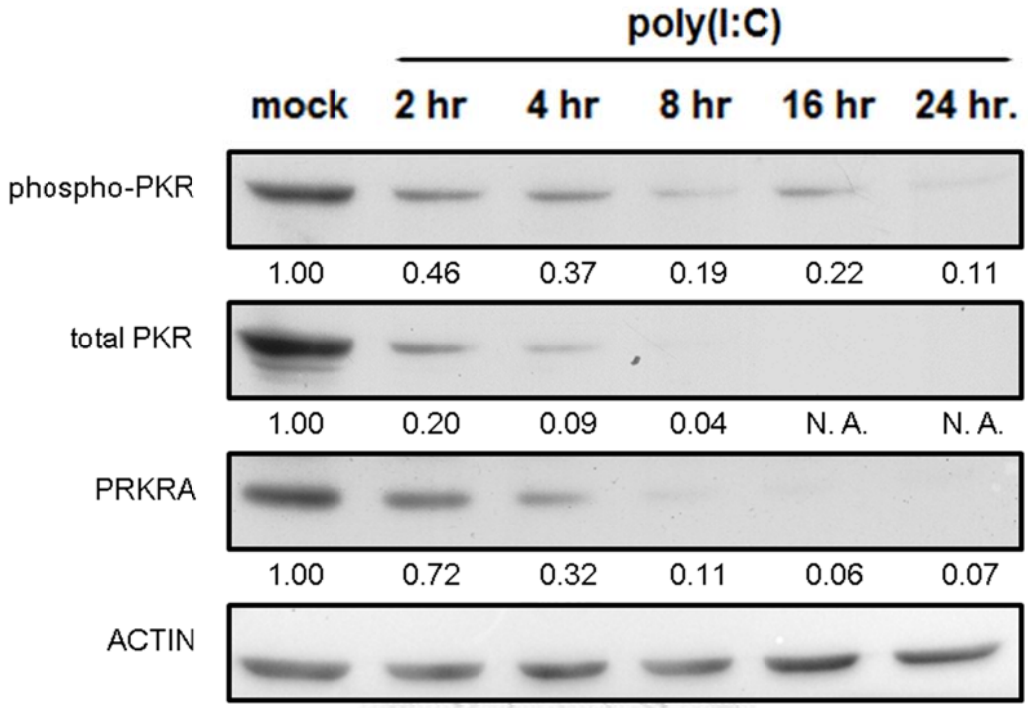

Figure 18. Protein expression of PRKRA was decreased gradually after poly(I:C) treatment.

SK-N-SH cells were transfected with poly(I:C) for 0, 2, 4, 8, 16 and 24 hours, and cell lysates were harvested by WCE buffer. The ratio of phospho-PKR to total PKR was gradually increased, but protein expression of PRKRA, PKR and phosphor-PKR were decreased.

7. Tables

Table 1. Specific primers of candidate target genes for qPCR				
No.	Gene Name	target	Forward or reverse	Primer sequence from 5' to 3' end
1	eEF1α	mRNA	F	TCGTGGGCGTGAACAAAATG
			R	GCTGACTTCCTTGACGATCTC
2	ADAR1	mRNA	F	GTTACCGCAGGGATCTACTGAGACT
			R	GACACACCCTAATCCATCTGTCACT
3	IFNAR1	mRNA	F	ATTTACACCATTTCGCAAAGCTC
			R	TCCAAAGCCCACATAACACTATC
4	IFNAR1	Edited fragment	F	ACATACACGTGTCTGCAG
			R	ATGAAAATGTGTCACCATG
5	IFNAR2	mRNA	F	TCATGGTGTATATCAGCCTCGT
			R	AGTTGGTACAATGGAGTGGTTTT
6	IFNAR2	Edited fragment	F	TCTCTGCATCCTAACTTGCTG
			R	AATGTGCATAGGTGATGTCAC
7	IFI27L1	mRNA	F	CTGTGGTCGGAGGAGTTGTG
			R	GGCGATTCCTACTGAGGTGAA
8	IFI27L1	Edited fragment	F	ATTGAATGGCTTAAAACAACAG
			R	ATGGAACATTCTCCTGAAGG
9	IFI27L1	Edited fragment	F	AAAGACACAGAGATTGGAGTG
			R	AAGTCCACAATCCAGGAGTC
10	PRKRA	mRNA	F	AGTAAGAAGCTGGCGAAACATAG
			R	TCAGGCATTAAGGGGTCAGGA
			R	ATCAAGTTCCATTGGCTCTGG

Table 1. Specific primers of candidate target genes for qPCR				
No.	Gene Name	target		Primer sequence from 5' to 3' end
11	Antisense of PRKRA	Edited fragment	F	ATTTCTCAAATAGGCTCAAC
			R	TCACTTATCACTTAATGGATG
12	MAVS	mRNA	F	CCTAAGGCCCTCTCTTTGCT
			R	GCACCTCCAAAGAGCTTGAC
13	MAVS	Edited fragment	F	GTTCCAGCTACTCAGGAGGC
			R	CACACTGGGCAGAGATGTGT
14	IRS-1	mRNA	F	TGTAGCAACGTGTGGTATGGC
			R	TTGAAGCATCAGCAAACCTTG
15	HLA-DRα	mRNA	F	TCTGGCGGCTTGAAGAATTTG
			R	GGTGATCGGAGTATAGTTGGAGC
17	PKR	mRNA	F	TCAGTGAAATCTGACTACCTGTCC
			R	ATGATTCAGAAGCGAGTGTGC
18	IFNB1	mRNA	F	TGTCAACATGACCAACAAGTGTC
			R	TAGGAATCCAAGCAAGTTGTAGC
19	N-Myc	mRNA	F	TGATCCTCAAACGATGCCTTC
			R	GGACGCCTCGCTCTTTATCT
20	EGR-1	mRNA	F	ACCCCTCTGTCTACTATTAAGGC
			R	TGGGACTGGTAGCTGGTATTG

Table 2. Specific primers of candidate target genes for end-point PCR				
No.	Gene Name	target	Forward or reverse	Primer sequence from 5' to 3' end
1	IFNAR1	Edited fragment	F	GTCATTGAGGAGACCCAGGA
			R	TTTCCCAGTGGTGAACACAG
2	IFNAR2	Edited fragment	F	CGTCTGCAAGTGTTCTCCAA
			R	CCCTTCTCTCCACTGCTCAC
3	IFI27L1-1	Edited fragment	F	GCACTGAGTTCAGGGAGAGG
			R	AGCCACAAGGCAAGGACGT
4	IFI27L1-2	Edited fragment	F	GCTGTCTTCTGGTTGCCTTC
			R	TGGGATTTCTGAGCTCTGTC
5	JAK2-1	Edited fragment	F	CAGTCTGAGATAGCTGCCAGA
			R	AAGGCTGTCCTTGCTGG
6	JAK2-2	Edited fragment	F	CCAGCAAGGACAGCCTT
			R	CAAACTCGGTTGGAGAGAC
7	JAK2-3	Edited fragment	F	GAAGCAGGTGGCCAATAAC
			R	GCAGCTGAAAGCACCATCT
8	MAVS-1	Edited fragment	F	CTCTCACCAGCTCTGTGACCT
			R	GCCCAGTGGACATACCTCTCT
9	MAVS-2	Edited fragment	F	GCCTGAGGTCTGGAGTTCAAG
			R	TCTCCCATCATGGCTGGTTACT
10	MAVS-3	Edited fragment	F	CTGGAGCGAAGTGGTGCAATC
			R	GGGTTTGGGTGCAGTGTCTCA

Table 2. Specific primers of candidate target genes for end-point PCR				
No.	Gene Name	target	Forward or reverse	Primer sequence from 5' to 3' end
11	PRKRA-1	Edited fragment	F	ATAATTGATCTATGCCAGGCTGG
			R	TTCAGGCTATACAGAAACAGCATG
12	PRKRA-2	Edited fragment	F	TTAGAAAGAAATGCGTAGGACCAC
			R	TAGTAAAGCAGCACACCCTTGC
13	PRKRA-3	Edited fragment	F	TCCTGATATTCTGTGCTACTTTGG
			R	ATTGGATGAATGGTCTCTCATCAG
14	PRKRA-4	Edited fragment	F	TTGAGACGGAGTATTGTTTCTGTTG
			R	AATTAGGTGGGTGTGGTGGC
15	PRKRA-5	Edited fragment	F	ACTACTGCTGTGTGCCACCAC
			R	ATCTTTCTGTGGTTGGATAGGG
16	PRKRA-6	Edited fragment	F	ATGCCTCTGAAACATTTCTTCC
			R	ACCAGCAACGTGTAAGGTTCC
17	RIG-1	Edited fragment	F	TGTAGCAACGTGTGGTATGGC
			R	TTGAAGCATCAGCAAACCTTG
18	STAT1	Edited fragment	F	CAGTTACCCGTGGTGCAGA
			R	GGTCAGATCACACTTGTTCCC